SEPARATION BY ADSORPTION METHODS

Theodore Vermeulen

Department of Chemical Engineering, and Radiation Laboratory,
University of California, Berkeley 4, California

I. General Survey

A. Introduction

The emergence of chemical engineering as a professional field of specialized knowledge was catalyzed to a major extent by the systematic classification of apparatus in terms of the Unit Operations. With further progress, the design methods evolved for particular apparatus types have proved equally applicable to other unit operations similar in physical arrangement, material and energy balances, rate behavior, and phase equilibrium. Thus there has been a very extensive development of parallel calculation methods for the separation operations conducted under countercurrent flow conditions—the fluid-fluid operations of distillation, absorption, and extraction.

Among the unit operations, adsorption may be considered a prototype for all fluid-solid separation operations. When it is conducted under countercurrent conditions, the calculation methods required are entirely analogous to those for countercurrent absorption or extraction (H3). Often, however, it is most economical to conduct adsorption in a *semicontinuous arrangement*, in which the solid phase is present as a *fixed bed* of granular particles. The fluid phase passes through the interstices of this bed at a constant flow rate and for an extended period of time. The concentration gradients in the fluid and solid phases display a transient or unsteady-state behavior, and their evolution depends upon the pertinent material balances, rates, and equilibria.

Figure 1 illustrates the two basic methods of fixed-bed operation. In *saturation*, the solute undergoing adsorption is removed continually from the carrier liquid or gas, and accumulates in the solid phase. Such transfer can continue until the concentration on the solid reaches a value corresponding to equilibrium with the concentration in the feed stream, and the column effluent reaches the feed concentration. When the column is saturated to the extent that "breakthrough" of the solute occurs, the flow is interrupted, and the column is then regenerated or eluted by pass-

ing through a stream, free of the solute in question, under conditions which favor desorption of this solute.

In elution separation, or *chromatography*, which also is shown in Fig. 1, only a small amount of solution containing the components to be separated is admitted to the column. These solute components are then carried through (eluted) by a carrier phase (the elutant) that initially is free of them. The solutes travel through the column as bands or zones at slightly different velocities. If the column is long enough, the zones will draw apart completely from one another, and may be recovered in the effluent as separate solutions of each individual solute.

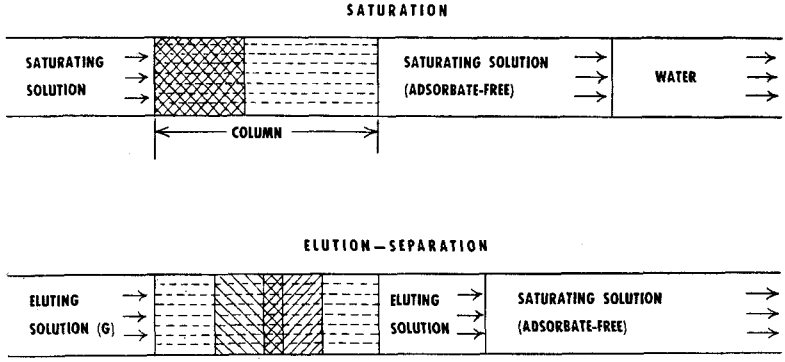

FIG. 1. Schematic diagrams for flow through a fixed-bed adsorption column. Courtesy of *Industrial and Engineering Chemistry*.

The techniques of laboratory- and industrial-scale separations utilizing adsorption and ion exchange have been described comprehensively by Mantell (M3), Cassidy (C2), and Nachod (N1). Treybal (T4) has recently provided a unified and modern chemical engineering approach to fluid-solid separation operations. The present article will treat the problems of data interpretation and apparatus design more extensively than the authors cited, and will give major emphasis to fixed-bed operations.

B. Fluid-Solid Transfer Operations

1. *Adsorption*

The term "adsorption operations," as used in this chapter, is intended to refer to all methods of separation that can be carried out with arrangements of apparatus characteristic of adsorption, or appropriate to it. Any separation operation based upon fluid-solid contact is thus somewhat related to adsorption, and the calculation methods developed for adsorption may prove applicable to it.

Adsorption is analogous to selective condensation of gas molecules or to selective crystallization or fusion from a liquid. It is based upon intermolecular attractive forces of the van der Waals type between a solute and the solid surface. These attractive forces will be most effective and most selective in a region adjacent to the surface and only one solute molecule thick (the monomolecular layer, or monolayer). Although multilayer deposition may develop as the concentration of solute increases toward a condition of normal condensation or precipitation, in general only monolayer adsorption will be involved and the available surface will not even be covered completely.

Since very large surface areas are usually needed, the solids used should be highly porous.[1] The extent of surface involved can be estimated from measurements of adsorptive capacity. With *n*-butyl amine as adsorptive,[2] for an example, the total volume occupied by one molecule (as liquid) is 1.65×10^{-22} cm.^{3} The area occupied by one molecule is approximately the two-thirds power of the volume, or 3.0×10^{-15} cm.^{2} An efficient adsorbent in contact with a gas phase may hold a volume of adsorbate equal to as much as 1.0% of the particle volume (silica gel has an even larger capacity). One cm.^{3} of such an adsorbent would thus present a surface area of 18 square meters, equivalent to about 5.5×10^6 square feet per cubic foot of particle volume. The precise value of the surface area will vary with the adsorptive species used for the measurement (B12).

The pore structure of catalysts, which is common to adsorbents generally, has been discussed in recent papers by Wheeler (W4).

In the broad sense, adsorption is the selective accumulation of chemical species at all types of phase interfaces. However, only the adsorption of solutes from a fluid phase (gas or liquid) onto a fluid-solid interface will be dealt with here. Such separation methods as froth flotation (D1) and foam fractionation (S3) will not be considered.

2. *Ion Exchange*

Ideally, an exchanger will alter the ionic composition of a solution without changing its over-all concentration of dissolved salts. The exchange material contains either cations or anions that can be displaced by other ionic species of like charge. Ion exchange may be written as a reversible chemical reaction; for example,

[1] In this chapter, a *pore* is an element of intraparticle space unfilled by crystalline material, while a *void* is an element of interparticle space in the packed bed.

[2] The *adsorptive* is the solute species undergoing adsorption. Cassidy (C2) reserves the term "adsorbate," often used in the same sense, to denote the combination of adsorbent and adsorptive.

$$Ca^{++}\ (aq.) + 2\ H^{+}\ (resin) \rightleftharpoons Ca^{++}\ (resin) + 2\ H^{+}\ (aq.)$$

or

$$Ca^{++} + 2\ HR \rightleftharpoons CaR_2 + 2\ H^{+}$$

where R^- or resin represents a stationary anionic site in the polyelectrolyte network of the exchanger phase.

Two distinct kinds of exchange materials have commercial importance. The first comprises claylike materials of high porosity, also called zeolites. The second consists of organic "resins," high-polymer materials which are homogeneous but permeable to water. The diffusional behavior is

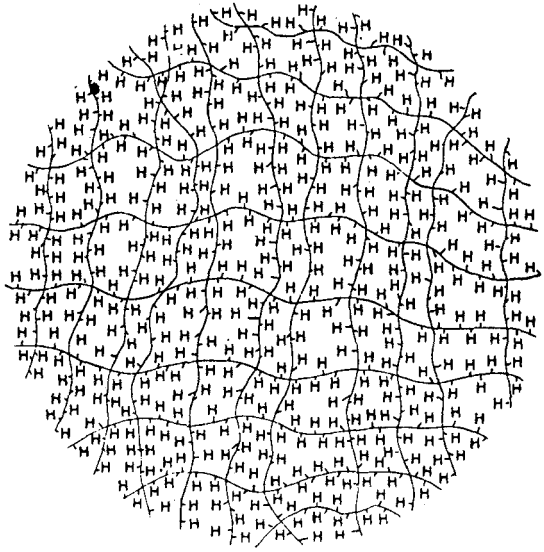

FIG. 2. Structural distribution of exchangeable ions in a synthetic organic resin after W. C. Bauman [p. 50 of reference (N1)].

different for these two kinds of exchanger, the first involving *pore diffusion* and the second homogeneous *intraparticle diffusion*. A schematic structural model of a submicroscopic ion exchange particle (of either kind), as visualized by Bauman and Eichhorn (B4), is given in Fig. 2.

The chemical properties of ion exchange resins are described fully in books by Kunin and Myers (K7) and by Nachod (N1), which give a general technical basis for selecting ion exchange materials for particular applications.

3. *Other Operations*

The theory presented in this article will apply directly to adsorption and to ion exchange operations. A number of related operations can also

be conducted under fixed-bed conditions, and their calculations will be closely analogous to those for adsorption. The similarities of these operations to adsorption will be traced qualitatively. The design calculations for these operations will not be treated separately.

a. Fixed-Bed (Partition) Absorption or Extraction. A porous granular solid may have its pores entirely filled with a liquid immiscible with, or nonvolatile in, the fluid to be processed. If the fluid is gaseous, its treatment by the impregnated solid conforms to the definition of absorption; and, if liquid, to extraction. The treating liquid is immobilized by its solid support, and the two in combination are used only in fixed-bed operation. The calculations for such an operation are wholly analogous to those for adsorption.

Partition chromatography (M4) is an elution-separation operation conducted over such a supported liquid-phase treating agent. Vapor-phase partition chromatography (or "gas chromatography") has recently undergone extensive development as an analytical tool. Fredericks and Brooks (F1) deal with its application to hydrocarbon mixtures, and Keulemans (K2) provides a comprehensive report on its uses.

Another instance of fixed-bed absorption or extraction is encountered in small-scale industrial operations, where trace impurities are to be removed from a process stream (for example, hydrogen sulfide from a refinery naphtha). The contacting tower may be filled intermittently with treating liquid, which remains in place during passage of the process stream until it is nearly spent. If no longitudinal mixing of the treating liquid occurs, the performance will be comparable to that of other fixed-bed operations. If longitudinal mixing does occur, a mathematical solution can be derived on the assumption that the mixing is perfect.

b. Leaching. This operation differs from simple dissolution, in having part of the solid phase insoluble in the solvent used for treatment. Its mathematical analysis is analogous to that for adsorption, where the external structure of the solid remains intact during the treatment. Practical examples of leaching are the treatment of such materials as ground sugar beets, ground roasted coffee berries, ores, or freshly formed filter cakes.

c. Drying of Solids. This operation, analogous to leaching, involves the removal of water or another volatile liquid, as vapor in an inert carrier gas. A frequent complication in the drying of vegetable or fruit materials is a decrease in diffusion rates due to shrinkage of pores as the drying proceeds (V1). When this occurs, the mathematical equations for adsorption operations will not apply, although their derivation may provide a model for handling this more complex case.

d. Regenerative Heat Transfer. This operation is commonly conducted

by heating a brick checkerwork with hot flue gases until it approaches the entering gas temperature, then cycling a process gas through the checkerwork to raise it to nearly the same temperature. The mathematical treatment of this fixed-bed operation (A3) has served as a model for the linear-equilibrium cases of adsorption (H7) and ion exchange (B5, B8, T2). The cyclic deposition and removal of thermal energy, with its attendant temperature gradients in the fluid and solid phases of the bed, is closely analogous to the deposition and removal of matter in a cyclic or "regenerative" operation.

e. Batch Distillation in a Packed Column. The kettle of a batch still provides the column with vapor feed, and the reflux condenser provides it with liquid feed. If the vapor and liquid feeds were exactly equal, the column would be maintained in a steady state, at total reflux. However, a small net flow of vapor is superposed upon the large refluxing flows. The transient distribution of concentrations in the column under this net flow is comparable to that produced in fixed-bed adsorptions. For example, the separation of two components having constant relative volatility and nearly equal molal volumes, corresponds to binary ion exchange with a moderately nonlinear equilibrium. Because the vapor feed to the column is of changing composition, the problem needs to be treated by the methods of Amundson (A2). The details of the correspondence of variables have not yet been worked out. In the general case, the feed composition will itself depend upon a material balance involving the overhead product composition.

II. Physical Factors Affecting Separation Performance

A. Equilibrium

1. *Types of Equilibria*

In designing adsorption equipment, the factors to consider are equilibrium, stoichiometry capacity, physical state (size, shape, and manner of packing) of the solid adsorbent, and rates controlling the separation. These subjects will be treated here only from the applicational viewpoint.

First, a number of relations will be considered expressing q^*, the equilibrium concentration in moles of adsorptive per unit weight of solid phase, as a function of c, the concentration in moles per unit volume of fluid phase. For adsorption from a gas, the partial pressure of adsorptive, p, may replace c.

The curve representing this function applies to conditions of constant temperature and is therefore known as an "adsorption isotherm." Three major classes of isotherms can be characterized by their different effects

upon column performance. DeVault (D2) first identified the "favorable" equilibrium for which the isotherm is convex upward (Fig. 3a); and the "unfavorable" equilibrium for which the curve is concave upward (Fig. 3b).[3] An intermediate case is that of the linear isotherm.

The slope of a favorable isotherm is thus a decreasing function, while the slope of an unfavorable isotherm is an increasing function, of c. It will be shown later that the equilibrium constants describing the isotherms are numerically larger in "favorable" than in "unfavorable" cases. In fixed-bed adsorption, favorable equilibria lead to relatively sharp concentration gradients in the direction of flow, while unfavorable equilibria lead to more diffuse boundaries.

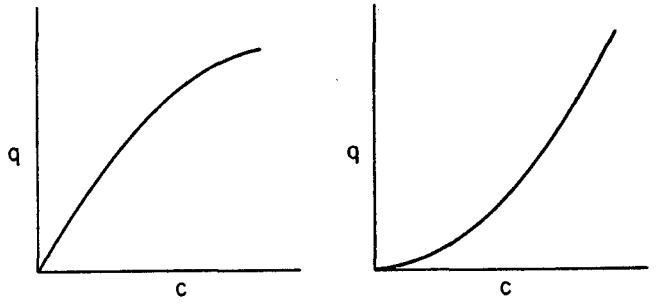

FIG. 3. Representative adsorption isotherms.

Isotherms having an inflection point correspond to ranges of both favorable and unfavorable equilibrium. Since separation operations only involve the part of the isotherm which lies below the feed-concentration, the occurrence of an inflection point corresponding to a higher concentration has no effect. If the inflection point occurs at a lower concentration, fixed-bed separation calculations must be carried out by approximate methods to be described below.

For fixed beds, simplified methods of calculation are available when the equilibrium can be considered highly favorable, highly unfavorable, or linear. The general case of nonlinear equilibrium has been solved for only a few types of equilibrium equations (Section II, A, 3). The discussion immediately following (Section II, A, 2) gives a wide selection of equilibrium relationships which can be used empirically in cases allowing the algebraic calculation of column performance; such cases are identified by italicized "type" descriptions.

[3] The terms "favorable" and "unfavorable," not used by DeVault, arise particularly from the consideration of ion-exchange equilibria.

2. *Equations for Highly Favorable or Highly Unfavorable Isotherms*

Research on adsorption as a method of determining surface areas of catalysts has led to the most general equilibrium relations yet available for representing *adsorption from the gas phase,* as developed by Brunauer and co-workers (B13). The widely used Brunauer-Emmett-Teller (BET) equation is

$$\frac{q^*}{q_m} = \frac{K_B p}{[P + (K_B - 1)p][1 - (p/P)]} \tag{1}$$

Here q_m is the adsorbate concentration when a monomolecular layer has been completely adsorbed; P is the vapor pressure of the pure adsorptive at the temperature of the isotherm, and K_B is an appropriate constant. This equation fits two types of isotherms (the type numbers given are Brunauer's, and the reader is referred to his article for graphic illustrations):

Type 2. Favorable at low, and unfavorable at high, concentrations (if $K_B > 1$).
Type 3. Unfavorable throughout (if $K_B < 1$).

A more general but highly complicated equation of essentially the same nature (B14) serves also to fit two other types of isotherms:

Type 4. Favorable at low and high concentrations, unfavorable at intermediate concentrations.
Type 5. Unfavorable at low, and favorable at high, concentrations.

Empirical equations of intermediate complexity also can be devised to fit isotherms of Types 4 and 5 in any particular instance.

When only monomolecular adsorption is involved, the BET relation (Eq. 1) reduces to the familiar Langmuir isotherm. With $p \ll P$, and $K_B \gg 1$, it becomes (L1)

$$\frac{q^*}{q_m} = \frac{K_L p}{1 + [K_L - (1/P)]p} \approx \frac{K_L p}{1 + K_L p} \tag{2}$$

where K_L replaces K_B/P. This relation corresponds to

Type 1. Favorable throughout.

Equations 1 and 2 both are based on the assumption that the enthalpy of adsorption does not change as p and q increase. For a particular distribution of enthalpy values, Sips (S5) has developed the following isotherm

$$\frac{q^*}{Q_\infty} = \left[\frac{K_S p}{P + (K_S - 1)p}\right]^M \tag{3}$$

Here Q_∞ is the concentration reached when the solid is saturated with liquid solute, the constant M characterizes the enthalpy distribution,

and K_S is another constant. On strictly empirical grounds, Koble and Corrigan (K5) have proposed a closely related equation which will sometimes be easier to use (N and K_C are empirical constants):

$$\frac{q^*}{Q_\infty} = \frac{K_C p^N}{P^N + (K_C - 1)p^N} \tag{4}$$

The foregoing two equations correspond to the following types of isotherm:

Type 1. Favorable throughout (if $M < 1$ and $M < 2K_S - 1$, or $N < 1$ and $N < K_C/[2 - K_C]$).

Type 2. Favorable at low, and unfavorable at high, concentrations (if $M < 1$ or $N < 1$ only).

Type 3. Unfavorable throughout (if M or N is greater than both criteria).

Type 5. Unfavorable at low, and favorable at high, concentrations (if $M > 1$ or $N > 1$ only).

With $K_S p$ or $K_C p^N \ll 1$, Eqs. (3) and (4) both reduce to the Freundlich relation (n and K_F are arbitrary constants):

$$q^* = K_F p^n \tag{5}$$

This corresponds to Type 1 (if $n < 1$) or Type 3 (if $n > 1$).

The foregoing equations appear to apply whether or not inert carrier gases are present. Regardless of the total pressure (so long as an ideal gas mixture is approximated), only the partial pressure of adsorptive affects the equilibrium. In *adsorption from the liquid phase,* it is generally necessary to assume that the solid is wetted by all the components of the liquid phase, and that all such components are adsorbed to an appreciable extent. For a two-component liquid, designating by N the mole-fraction of the component under consideration, isotherms similar to Eqs. (1–5) can be used on an empirical basis:

$$\frac{q^*}{Q_\infty} = \frac{K_B' \mathrm{N}}{[1 + (K_B' - 1)\mathrm{N}][K_B'' + (1 - K_B'')\mathrm{N}]} \tag{6}$$

$$\frac{q^*}{Q_\infty} = \frac{K_L' \mathrm{N}}{1 + (K_L' - 1)\mathrm{N}} \quad \text{or} \quad \frac{(1 + K_L'')\mathrm{N}}{1 + K_L'' \mathrm{N}} \tag{7}$$

$$\frac{q^*}{Q_\infty} = \left[\frac{(1 + K_S')\mathrm{N}}{1 + K_S' \mathrm{N}}\right]^M \tag{8}$$

$$\frac{q^*}{Q_\infty} = \frac{(1 + K_C')\mathrm{N}^m}{1 + K_C' \mathrm{N}^m} \tag{9}$$

$$q^*/Q_\infty = \mathrm{N}^n \tag{10}$$

Two additional forms will sometimes prove useful. The first is

$$\frac{q^*}{Q_\infty} = \frac{\mathrm{N}^l}{\mathrm{N}^l + K(1 - \mathrm{N})^l} \tag{11}$$

where l is a suitable constant. Equation 11 can represent the following types of behavior:

Type 1. Favorable throughout ($l = 1$, $K > 1$).
Type 2. Favorable at low, and unfavorable at high, concentrations ($l < 1$).
Type 3. Unfavorable throughout ($l = 1$, $K < 1$).
Type 5. Unfavorable at low, and favorable at high, concentrations ($l > 1$).

Another form is a power-series expression which can be made to conform to any of the five shapes of isotherm that have been discussed here:

$$q^*/Q_\infty = (1 + A + B + C)\mathrm{N} - A\mathrm{N}^2 - B\mathrm{N}^3 - C\mathrm{N}^4 \qquad (12)$$

Any two terms of Eq. (12) can only correspond to either Type 1 or Type 3. Any three terms, potentially, can give Type 2 or Type 5. The sum of four terms may give a satisfactory fit to a Type 4 isotherm (initially favorable, later unfavorable, finally favorable).

An isotherm which is markedly favorable or unfavorable may be approximated by a line or curve intercepting either of the positive axes. Thus, Eagleton and Bliss (E1) used a relation of the type:

$$q^*/Q_\infty = A + (1 - A)\mathrm{N} \qquad (13)$$

If A is positive, the isotherm can be considered favorable throughout; if negative, unfavorable throughout; and if zero, linear.

When a non-ideal binary liquid solution is equilibrated with a solid whose adsorption sites are all identical, a mass-action equilibrium expression can be written which contains the activity coefficients (γ_A and γ_B) of the liquid components:

$$K = \frac{q_\mathrm{A}^*\mathrm{N}_\mathrm{B}\gamma_\mathrm{B}}{q_\mathrm{B}^*\mathrm{N}_\mathrm{A}\gamma_\mathrm{A}} \qquad (14)$$

The activity coefficients for these species in the solid phase are of course included in the equilibrium constant. This can be shown to reduce to Eq. (7) when $\gamma_\mathrm{A} = 1$ and $\gamma_\mathrm{B} = 1$ throughout. In general, the activity coefficients are given approximately by

$$\begin{aligned} \gamma_\mathrm{A} &= e^{L\mathrm{N}_\mathrm{B}^2} \\ \gamma_\mathrm{B} &= e^{L\mathrm{N}_\mathrm{A}^2} \end{aligned} \qquad (15)$$

where L is a symmetric or "two-suffix" Margules coefficient. For a homogeneous solution with positive deviations from Raoult's Law, $0 < L < 2$. Combination of Eqs. (14) and (15) yields

$$\frac{q_\mathrm{A}^*x_\mathrm{B}}{q_\mathrm{B}^*x_\mathrm{A}} = Ke^{L(\mathrm{N}_\mathrm{B}^2-\mathrm{N}_\mathrm{A}^2)} \qquad (16)$$

With positive deviations from Raoult's Law, the partition ratio $q_\mathrm{A}^*/\mathrm{N}_\mathrm{A}$ for adsorption of a component will increase as its concentration decreases.

This corresponds to a Type 2 isotherm. Even if Eq. (16) correctly represents the equilibrium data, it is generally more convenient to fit the isotherm empirically by the use of Eq. (12), (11), or (6).

3. *Equations for Moderately Favorable or Moderately Unfavorable Equilibria —The Equilibrium Parameter*

Of the foregoing equilibrium expressions, only two, namely Eq. (2) (the Langmuir relation) and Eq. (7), have been utilized in a general treatment of adsorption rates.

Although these mass-action expressions are the most frequently used owing to their simplicity, it remains possible that rate treatments based on other equilibrium relations will be derived in the future.

In applying the Langmuir relation to column calculations, the ratio q^*/q_m will be less important than the ratio q^*/q_o^*, where q_o^* is the *maximum* concentration that can be reached in the column, i.e., the solid concentration in equilibrium with the inlet solution concentration p_o. From Eq. (2),

$$\frac{q^*}{q_o^*} = \frac{(1 + K_L p_o)p}{(1 + K_L p)p_o} \tag{17}$$

Use may be made of a dimensionless *equilibrium parameter*, $\mathbf{r}$, defined in this case as

$$\mathbf{r} = \frac{1}{1 + K_L p_o} \tag{18}$$

In terms of $\mathbf{r}$, the isotherm becomes

$$\frac{q^*}{q_o^*} = \frac{p/p_o}{\mathbf{r} + (1 - \mathbf{r})(p/p_o)} \tag{19}$$

Eq. (7) may be put into the same form by using as the equilibrium parameter

$$\mathbf{r} = 1/K_L' \tag{20}$$

with the result that

$$\frac{q^*}{Q_\infty} = \frac{\mathrm{N}}{\mathbf{r} + (1 - \mathbf{r})\mathrm{N}} \tag{21}$$

From Eq. (21), the parameter $\mathbf{r}$ is found to be analogous to the *relative volatility* used in distillation calculations:

$$\mathbf{r} = \frac{\mathrm{N}(Q_\infty - q^*)}{q^*(1 - \mathrm{N})} \tag{22}$$

Thus $\mathbf{r}$ may also appropriately be called the "separation factor."

The only available general treatment of adsorption rates is based upon

Eqs. (2) and (7) as equilibrium expressions, and thus assumes a *constant separation factor.*

As has already been indicated, any separation involves only the part of the isotherm which lies at or below the feed-concentration level. An empirical fit, based upon the assumption of a constant separation factor, can often be made to this part. For this purpose, Eq. (7) can be rewritten in the form

$$\frac{q^*}{Q} = \frac{K(c_A)_o}{C_o + (K-1)(c_A)_o} \tag{23}$$

where, for empirical use, C_o and Q are regarded as adjustable parameters rather than measured constants for the system. Figure 4 is a logarithmic

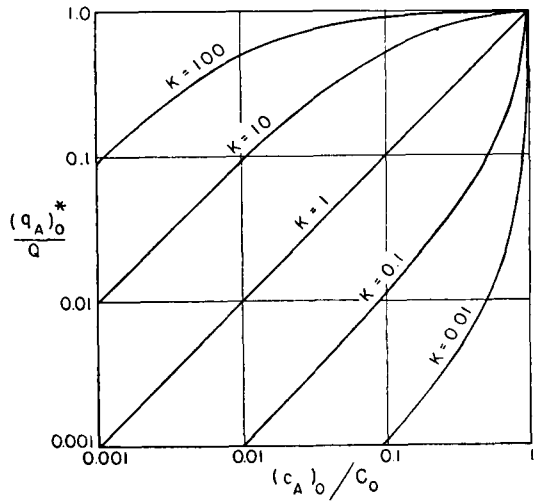

FIG. 4. Dependence of isotherms upon equilibrium constant. The log-log scale is useful for empirical matching with experimental isotherms. Courtesy of *Journal of Chemical Physics* (V5).

plot of Eq. (23). Any isotherm plotted on similar coordinates which shows either a steadily decreasing or a steadily increasing slope can be matched approximately to one curve of this family, and can be described using appropriate values of K, C_o, and Q (V5). An experimental plot of c vs. q is prepared on an identical logarithmic grid. This plot is superposed upon the master plot by sliding it in both coordinate directions until the best fit is obtained to a portion of one of the master-plot curves. The coordinates of the master plot corresponding to $c = C_o$ and $q = Q$ are traced onto the experimental plot, so as to provide the proper numerical values of C_o and Q. The value of K is read directly from the curve

which gives the best fit. The equilibrium parameter for this isotherm, as developed in the reference article (V5), is:

$$\mathbf{r} = \frac{C_0}{(K-1)(c_A)_o + C_o} \tag{24}$$

If an isotherm fits Fig. 4 exactly all the way to $(c_A)_o/C_o = 1$, C_o corresponds to the true total solution concentration and Q to q_o*. Equation (24) then becomes applicable to a *binary mixed feed*, to be described (Section III, D, 1b).

It will be seen that $\mathbf{r} = 1$ corresponds to the *linear isotherm*. Under certain conditions many of the isotherms considered in the preceding section also become linear.

4. *Isotherms Partly Favorable and Partly Unfavorable*

Algebraic relations for equilibria that are partly favorable and partly unfavorable are included in Section II, A, 2. Such relations can sometimes be used for separation calculations where only the highly favorable part of the isotherm, or only the highly unfavorable part, is involved. In all other such cases the equilibrium data can be utilized numerically, by dividing the concentration range into several sections and determining an average $\mathbf{r}$ for each interval. The use of non-constant $\mathbf{r}$ values will be described in Section III, D, 4.

5. *Ion Exchange Equilibria*

The equilibria between *ions of equal valence* (homovalent ions) are usually represented by a simple mass-action relation, analogous to Eq. (7) or (22):

$$K(=K^{II}) = \frac{q_A c_B}{q_B c_A} \tag{25}$$

The use of this relation has been justified experimentally by Bauman and Eichhorn (B4) and by Boyd *et al.* (B9). For organic resin exchangers, Gregor (G7) has shown that K varies with changes in resin density that occur progressively during exchange. High concentrations in the solution phase lead to an appreciable uptake of unbound ions by the resin structure, and this uptake also affects the apparent equilibrium. Moreover, the thermodynamic activities of the exchanging ions in solution will change with changing ionic strength; for two ions of equal valence, the changes in activity coefficients frequently will be almost equivalent, and for such cases K will be nearly independent of the total ionic concentration of the solution.

Such factors as these make it difficult to obtain a completely general

relation for exchange between *ions of unequal valence* (heterovalent ions). A mass-action expression is again the best approximation. For the exchange

$$A^{(\alpha+)} + \frac{\alpha}{\beta} BR_\alpha \rightleftharpoons AR_\alpha + \frac{\alpha}{\beta} B^{(\beta+)}$$

the equilibrium relation is

$$K = \frac{q_A{}^\beta c_B{}^\alpha}{q_B{}^\alpha c_A{}^\beta} \tag{26}$$

or

$$K \left(\frac{Q}{C_o}\right)^{\alpha-\beta} = \frac{(q_A/Q)^\beta (c_B/C_o)^\alpha}{(q_B/Q)^\alpha (c_A/C_o)^\beta} \tag{27}$$

where Q $(= q_A + q_B)$ is the total exchange capacity of the solid, and C_o $(= c_A + c_B)$ is the total concentration of ions in solution. For the case

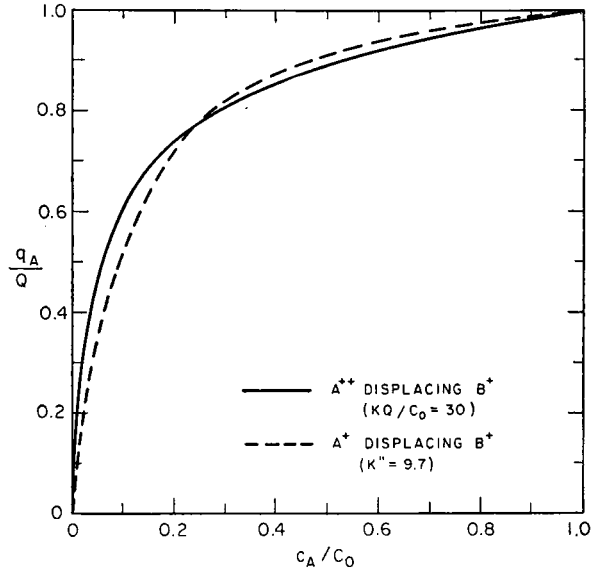

FIG. 5. Typical equilibrium distribution of heterovalent ions between solution and resin, showing its approximation by a second-order equilibrium constant (K^{II}) equivalent to a constant separation factor. Courtesy of *Chemical Engineering Progress* (H6).

of unequal valences, concentrations should be expressed in equivalents rather than in moles.

Data obtained by Gregor (G7) suggest that some complex-ion formation occurs in the resin, of the type

$$A^{(\alpha+)} + X^- + \frac{\alpha - 1}{\beta} BR_\beta \rightleftharpoons AXR_{\alpha-1} + \frac{\alpha - 1}{\beta} B^{(\beta+)}$$

Walton (W2), and Kunin and Myers (K7), have reviewed the empirical equations that have been proposed to fit ion-exchange equilibria; many of these relate specifically to inorganic zeolites rather than to the synthetic-resin exchangers.

For rate calculations, the equilibrium may need to be represented by Eq. (25), as has been shown by Hiester and Vermeulen (H6). A suitable average value of K^{II} over the entire concentration range is given by

$$K^{II} = [K(Q/C_o)^{\alpha-\beta}]^{2/(\alpha+\beta)} \tag{28}$$

For *trace* concentrations of A, in the vicinity of $c_B = C_o$ and $q_B = Q$, the preferred relation (V4) is

$$K^{II} = [K(Q/C_o)^{\alpha-\beta}]^{1/\beta} \tag{29}$$

The nature of the approximation to Eq. (26) that is given by Eqs. (28) and (25) is shown in Fig. 5.

B. Stoichiometric Capacity

The adsorption or exchange capacity of a column will have a major effect upon the volume of the fluid which can be treated before breakthrough. The equilibrium isotherm for adsorption, as a general rule, will indicate the maximum uptake. For ion exchange (K7) the capacity specified by the manufacturer, or determined experimentally, often can be used without correction.

Occasionally, particularly in cases of high fluid-phase concentration, the capacity must be defined with some care. For material-balance purposes, a suitable boundary must be defined between the solid and the solution. Ordinarily this boundary is the outer surface of the particles. The "solid" concentration at equilibrium, q^*, includes fluid-phase solute in amount $c(1 - \epsilon)\chi$, where $(1 - \epsilon)$ is the non-void fraction and χ is the fractional internal porosity of the particles. The apparent equilibrium constants and particle diffusion rates may therefore vary with c and with χ; the mathematical treatment can be modified accordingly, when necessary.

The rate of uptake of large molecules by an adsorbent or exchanger may lead to apparent variations in capacity. Ion exchange of Dowex 50 in the hydrogen form, with *n*-butyl amine, indicated to Vermeulen and Huffman (V6) that the normal exchange capacity of the resin could be divided into relatively accessible (60%) and relatively unaccessible (40%) portions. A more likely interpretation, based upon work of Wilson and Lapidus (W8) and Gregor (G7), is that the resin-phase diffusivity declines sharply as the uptake of amine increases. For design calculations, however, it may be necessary to assume a reduced capacity.

The varying uptake due to heterovalence (G7) has been mentioned in Section II, A, 5. For the case of a divalent cation M^{++} and a univalent anion X^-, the complex-ion equilibrium might be represented by

$$\frac{q_{MX^+}{}^2}{q_{M^{++}}c_{X^-}{}^2 c_{M^{++}}} = K_{\text{complex}} \tag{30}$$

Boyd *et al.* (B8) have reported a variation in the capacity of Amberlite IR-1, a resin containing sulfonic, carboxylic, and phenolic groups.

The uptake of anions, as well as cations, by a cationic exchanger, is predicted by the Donnan theory of membrane equilibria, to increase with the electrolyte concentration in the external solution phase. The cations thus absorbed must be included in the effective resin capacity. Data of Bauman for the HCl uptake in Dowex 50, taken from an experimental plot (N1), are as follows:

Soln. (Cl^-), M	0.1	0.2	0.5	1	2	5
Resin (Cl^-), M	0.006	0.012	0.03	0.07	0.2	1.2

Resins with a low extent of cross-linking, which have a higher water content, will show a larger uptake of ions from the solution phase. Since the total resin concentration is around 7 M, the effect usually is negligible.

C. Rate Behavior

1. *Rate-Determining Mechanisms*

The sequence of molecular-scale processes involved in an exchange adsorption, in which species B initially adsorbed on the solid is displaced by species A initially in solution, can be grouped into the following four steps, as outlined by Klotz (K4):

a. Fluid-phase external diffusion, sometimes called film diffusion (or F mechanism). Counter-diffusion of A from the bulk fluid to the outer surface of the solid particle and of B from the particle to the bulk fluid.

The rate of material transfer of A into the particle may be expressed:

$$\frac{dq_A}{d\tau} = k_f a_p \frac{\epsilon}{\rho_b}(c_A - c_A{}^*) \tag{31}$$

where k_f is the fluid-phase mass-transfer coefficient, a_p is the external area of particles per unit bulk volume of packed column, ϵ is the fraction of external voids, τ is time, and ρ_b is bulk density of the packing.

b. Fluid-phase pore diffusion, in porous bodies whose pores are freely accessible to the bulk fluid outside. Counter-diffusion of A through the pores of the particle to the point where exchange occurs and of B from the point of exchange in the pore surface back to the outer surface of the particle.

The pore-diffusion rate for a sphere, as adapted from Barrer (B2), is

$$D_{\text{pore}}\left(\frac{\partial^2 c_i}{\partial r^2}+\frac{2}{r}\frac{\partial c_i}{\partial r}\right)=\chi\frac{\partial c_i}{\partial \tau}+\rho_p\frac{\partial q_i'}{\partial \tau} \tag{32}$$

where D_{pore} is the diffusivity, ρ_p is the density of the adsorbent particle, c_i is the fluid-phase concentration of component within the particle at radius r, and q_i' $(= q_i - \chi c_i)$ will generally be in equilibrium with c_i. The mean concentration of the entire particle, of total radius r_p, is

$$q=\frac{3}{r_p^3}\int_0^{r_p} q_i r^2 dr \tag{33}$$

Here r_p is the outer radius of the particle. These equations will normally be written in terms of the component being adsorbed. If exchange adsorption is involved, with consequent counter-diffusion, this will enter into the evaluation of D_{pore}.

c. Reaction, or Phase Change. Desorption of B from the solid phase at a pore surface or at the outer surface, and adsorption of A in its place.

For one-component adsorption, the rate is

$$\frac{dq_i}{d\tau}=k_i'\left[p(q_m-q_i)-\frac{1}{K_L}q_i\right] \tag{34}$$

For exchange between two components, usually from the liquid phase,

$$\frac{d(q_A)_i}{d\tau}=k_i\{c_A[(q_A)_o^*-(q_A)_i]-\mathbf{r}(q_A)_i(C_o-c_A)\} \tag{35}$$

Here q_i or $(q_A)_i$ is the solid-phase concentration at the surface, and k_i' or k_i is the rate of surface reaction. When the surface-reaction equation is used empirically for the entire rate behavior, k_i will be replaced by k_{kin}.

Equation 34 may be put into the form of Eq. (35). Use of Eq. (2) in the Langmuir form replaces q_m by q_o^*, and also introduces p_o; correspondence is obtained if $k_i = k_i'/(1-\mathbf{r})$ or $k_i' q_m/q_o^*$.

Surface reaction is usually very fast compared to the rates of material transfer, so that experimental values of k_i are not known.

d. Solid-phase internal diffusion, sometimes called particle diffusion or P mechanism. This includes diffusion through a homogeneous, permeable (i.e. absorbing), non-porous solid; diffusion in a mobile, adsorbed phase covering the pore surfaces of a porous solid whose crystalline portion is impermeable; or diffusion in an absorbing liquid held in the pore spaces of a solid.

The rate of internal diffusion is expressed by

$$D_p\left(\frac{\partial^2 q_i}{\partial r^2}+\frac{2}{r}\frac{\partial q_i}{\partial r}\right)=\frac{\partial q_i}{\partial \tau} \tag{36}$$

Here D_p is the diffusivity, and q_i is the solid-phase concentration at radius r. This equation has been solved only for the irreversible- and linear-equilibrium cases of fixed-bed operation (Sections III, B, 2 and III, C, 2). It is usually approximated by the linear-driving-force relation (G5)

$$\frac{dq_A}{d\tau} = k_p a_p (q_A^* - q_A) \tag{37}$$

where $k_p a_p$ ($= 60 D_p/d_p^2$) is the mass-transfer coefficient, q_A is the concentration of A averaged over the entire particle, and q_A^* is the concentration the particle would have if it were in equilibrium with the instantaneous, fluid-phase concentration at the outer surface of the particle.

The sequence of steps will be (a)-(c)-(d) in ion exchange with synthetic-resin materials, and in partition absorption or extraction. For simple adsorption (or ion exchange on inorganic zeolites) the sequence will usually be (a)-(b)-(c), occasionally (a)-(c)-(d), and rarely (a)-(b)-(c)-(d).

2. *Adsorption Rates*

a. Fluid-phase external diffusion rates appear to conform to the general mass-transfer correlations developed by (among others) Wilke and Hougen for gases (W6), and McCune and Wilhelm (M1) and Gaffney and Drew (G1) for liquids. Evidence of this general agreement has been provided by Dryden (D6), who found an additional resistance attributable to pore diffusion; Dodge and Hougen (D3); Eagleton and Bliss (E1); and others. The correlation of Wilke and Hougen, for example, is expressed in the present notation as

$$k_f = \frac{U}{H_f a_p} = 1.82 U \left(\frac{d_p U \epsilon \rho}{\mu}\right)^{-0.51} \left(\frac{\mu}{\rho D_f}\right)^{-0.67} \tag{38}$$

where U is the mean linear velocity, $U\epsilon$ is the superficial velocity, H_f the height of a transfer unit (or HTU), μ the viscosity of the fluid, ρ the density of the fluid, D_f the bulk diffusivity of the solute in the fluid, and d_p is the effective particle diameter.

b. Fluid-phase pore diffusion rates have been discussed extensively by Wheeler (W4) for the related problem of solid-catalyzed reactions. For diffusion in liquids, and in gases under high pressure, the pore diffusivity is given approximately by

$$D_{pore} = \frac{D_f \chi}{2} \tag{39}$$

For gases at ordinary pressures in fine pores, Knudsen-flow diffusion is encountered if the molecular mean free path is larger than the pore

radius. Wheeler's work gives a relation applicable to all combinations of bulk diffusion and Knudsen flow:

$$D_{\text{pore}} = \frac{D_f \chi}{2} (1 - e^{-2\bar{r}\bar{u}/3D_f}) \tag{40}$$

where the average pore radius $\bar{r}$ is given approximately by the ratio of particle volume to internal pore surface; and $\bar{u}$ is the average molecular velocity:

$$\bar{u} = (8RT/\pi M)^{1/2} \tag{41}$$

with R the gas constant per mole and M the molecular weight of the solute. At large ratios of mean free path to pore radius, the pore diffusivity becomes $2\chi\bar{r}\bar{u}/3$.

Calculations based solely upon a constant D_f do not include the effects of mass flow or of changing composition, but these will generally be negligible.

3. *Ion Exchange Rates*

For exchange in inorganic zeolites, the same rate relations should apply as for adsorption from a liquid phase.

With the synthetic-resin exchangers, the external mass-transfer rate again corresponds to Eq. (38). Data of a number of investigators (B8, G2, M7, N2, S4) have been reviewed by Hiester (H4), and have led to the construction of Fig. 6. The functions plotted, which will be discussed fully in Section III, D, 5, correspond to the relation

$$\frac{H_R D_p}{d_p^2 U} = \alpha_1 \left(\frac{D_f}{d_p U}\right)^{1/2} \frac{D_p}{D_f} + \alpha_2 \tag{42}$$

where H_R is an HTU based upon the reaction-kinetic mechanism, and α_1 and α_2 are constants. The horizontal section of the curve corresponds to internal diffusion and the sloping section to external diffusion. An earlier correlation was given by Vermeulen and Hiester [Fig. 6 of reference (V4)] based upon some of the same data; however, the channeling correction factor $(d_w/d_p)^{1/3}$ introduced there has proved generally to be unnecessary. This reference indicates that *longitudinal dispersion* will need to be considered at $(d_p U)$ values below 10^{-3} cm.^{2}/sec.

The D_p values for univalent cations in Amberlite IR-1, a sulfonated phenol-formaldehyde resin, are in the range of 2 to 3 $\times$ 10^6 cm.^{2}/sec., or about 0.15 times the diffusivity in solution (B8). For divalent cations values of 7 to 10 $\times$ 10^{-7} cm.^{2}/sec., and for trivalent ions values of 3 to 4 $\times$ 10^{-7}, are indicated by chromatographic runs on Amberlite

IR-1 (V4). The D_p values for Dowex 50, a typical sulfonated polystyrene resin, have been shown by Boyd and Soldano (B7) to depend greatly upon the extent of cross-linking as determined by the divinylbenzene (DVB) content of the resin. For 8% DVB, the D_p values are similar to Amberlite IR-1. For 12% DVB, the usual commercial grade, self-diffusion

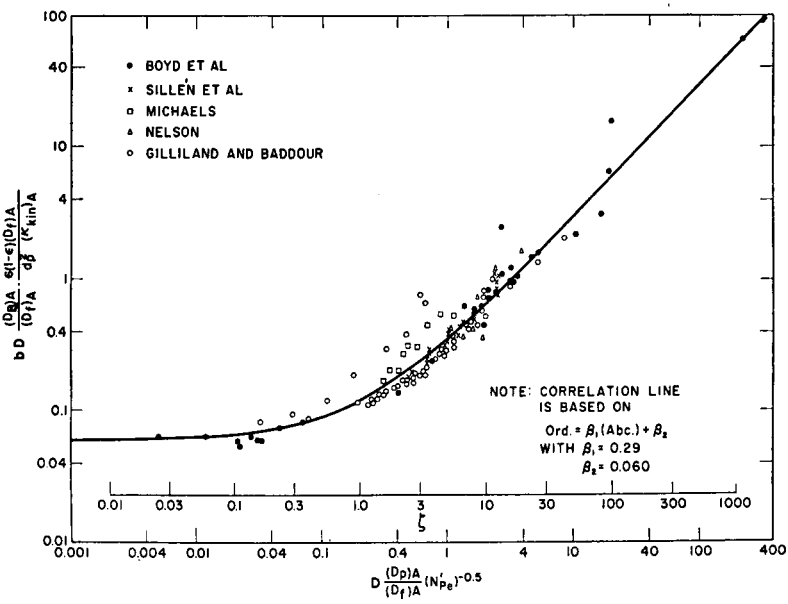

FIG. 6. Logarithmic correlation of ion exchange rates in fixed-bed columns. Courtesy of *A. I. Ch. E. Journal* (H4).

values at 25°C. are: Na^+, 2.9×10^{-7}; Zn^{++}, 2.9×10^{-8}; Y^{+++}, 3.2×10^{-9}; Th^{++++}, 2.2×10^{-10}. Data are also reported for a typical anionic exchanger (B7).

III. Binary Fixed-Bed Separations

A. Factors Common to All Cases

1. *Variables and Parameters*

Column performance studies for fixed-bed columns are concerned with the concentration history of the column effluent—that is, with the variation in concentration as a function of time or of volume of effluent. Concentration-history calculations for fixed-bed adsorption and ion-exchange columns must make use of one or another of a group of specialized results which take the place of a general solution to the problem. The specialized results can be identified on the basis of controlling mecha-

nism (external diffusion, internal pore diffusion, internal solid-phase diffusion, or longitudinal diffusion) and of equilibrium (unfavorable, linear, favorable, or completely irreversible).

The same principles are involved in two different types of operation: saturation, in which one or more solute components are separated from the solvent, and chromatography, in which two or more solute components are separated from one another. Saturation operations will be discussed in this section, and chromatography in the next. The terminology will be that adopted in previous papers by Vermeulen, Hiester, and co-workers (H1–6, V3–6).

The relative concentrations in the column and in the effluent depend upon several physical variables. Once the variables are defined and interrelated, the algebraic and numerical results can be given in relatively simple form. The successful development and design of adsorption operations involves the optimization of all the variables, through the use of equations or curves that really correspond to the physical situation. Unless the entire range of possible behavior is understood, the designer will risk using an inappropriate method. The principal variables are:

Column volume, v. For a point within (or at the downstream end of a column, v will be measured from the upstream end. If h is the height and S is the superficial cross-sectional area, $v = hS$. If ϵ is the void fraction for the column as packed, $v\epsilon$ is the effective volume of fluid in the column.

Volumetric flowrate, F. The residence time for fluid in the column is $v\epsilon/F$. The linear flowrate is given by $U = F/S\epsilon$, and the superficial flowrate is $U\epsilon = F/S$.

Fluid volume passing through the column. The fluid is assumed to enter the column with a sharp front, at time $\tau = 0$, and to flow at constant and uniform velocity. V is the volume that has entered the column up to a particular time τ. At that instant, $V - v\epsilon$ is the volume that has passed out of the column (of volume v) and $\tau - (v\epsilon/F)$ is the elapsed time as measured from the time of the initial arrival of the fluid front at the column exit.

Stoichiometric capacity of the column, $q_o^*\rho_b v$ for adsorption, or $Q\rho_b v$ for simple binary ion exchange. This variable has been discussed in Section II, B.

Material-transfer rates, as reviewed in Section II, C.

Particle diameter, d_p, *and pressure drop.* For a given column performance, the pressure drop is lowest when the adsorbent particles are spherical and of closely uniform size. The external mass-transfer rate increases inversely as $d_p^{3/2}$, and the internal rate increases inversely as d_p^2. The pressure drop variation will depend upon the Reynolds number, but is

about proportional to $U^{3/2}$ and also inversely to $d_p^{3/2}$. Pressure-drop relations are reviewed by Drew and Genereaux (D4), Brownell (B11), and Ergun (E3). In many instances increasing the pressure drop, by using a longer column of smaller diameter, will substantially improve the resin utilization.

The analytical or graphical solutions for concentration are usually obtained in a dimensionless form, which provides the greatest generality. This requires that the column and solution variables be assembled into the following dimensionless parameters:

a. Solution Concentration Ratio, **x**. The column calculations to be considered here usually involve a constant solute concentration in the feed, which can be taken as unity on a relative scale of concentration. The parameter **x**, based on this value, then expresses the ratio of solute concentration in the solution at any downstream point to the feed value; that is,

$$\mathbf{x}_A = c_A/(c_A)_o \tag{43}$$

If the entire system contains only one solute, the subscript is dropped

$$\mathbf{x} = c/C_o \tag{44}$$

If a two-component mixture is fed to a column containing one or both of the components, **x** will be replaced by λ as the corresponding variable (see Section III, D, 1b).

b. Solid Concentration Ratio, **y**. The solute concentration in the solid phase, that is reached after continued contact with successive portions of entering feed, is taken as unity on a relative scale. The parameter **y** then expresses the ratio of solute concentration on the solid to the maximum attainable concentration.

For adsorption of a single solute,

$$\mathbf{y} = q/q_o^* \tag{45}$$

In ion exchange,

$$\mathbf{y}_A = q_A/Q \tag{46}$$

or, alternatively,

$$\mathbf{y}_A = q_A/(q_A)_o^* \tag{47}$$

For a mixed binary feed, or for a column with uniform partial presaturation, **y** will be replaced by ω (Section III, D, 1b).

c. Equilibrium Parameter, or Separation Factor, **r**. For exchange adsorptions (Eqs. 7, 20, 22, 25), **r** is given by $(1/K_L')$ or $(1/K^{II})$. Simple relations express **r** in certain other instances of adsorption (Eqs. 18, 24).

d. Distribution Ratio, **D**. This is the limiting value reached as saturation is approached. For simple adsorption,

$$\mathbf{D} = q_o^* \rho_b / C_o \epsilon \tag{48}$$

For simple binary ion exchange,

$$\mathbf{D} = Q\rho_b/C_o\epsilon \tag{49}$$

This dimensionless ratio may be compared with K_d used by Boyd (B9), Mayer and Tompkins (M6), and others in the chemical literature on ion exchange. In their work, $K_d = Q/C_o$.

e. Number of Transfer Units, $\mathbf{N}$, *or* Σ. In fixed-bed operations, it is desirable to obtain a concentration history curve that is steep by comparison to the total volume of solution handled in any one cycle. For saturation, a steep breakthrough curve makes it possible to utilize a large fraction of the theoretical capacity of the resin. For chromatography, steep-sided zones provide bettter recoveries and purities of the individual components.

The relative steepness or "sharpness" improves as the volume of the resin bed increases and also as the exchange rate increases. In order to use generalized mathematical results, these two factors must be combined into a dimensionless column capacity parameter Σ, which is entirely analogous to the number of transfer units, NTU or $\mathbf{N}$, as defined by Chilton and Colburn for differentially continuous separations (C3).

For external diffusion controlling,

$$\mathbf{N}_f\ (= \Sigma_f) = k_f a_p v\epsilon/F \tag{50}$$

If pore diffusion contributes or controls, k_f is replaced by k_f'. For solid-phase internal diffusion controlling,

$$\mathbf{N}_p\ (= \Sigma_p) = k_p a_p \mathbf{D} v\epsilon/F \tag{51}$$

with $k_p a_p = 60 D_p/d_p^2$ as given by Glueckauf (G5). For both resistances appreciable, the over-all NTU's are

$$\mathbf{N}_{Of} = \frac{\mathbf{b}_f v\epsilon}{\left(\frac{1}{k_f a_p} + \frac{1}{k_p a_p \mathbf{D}}\right) F} \tag{52}$$

$$\mathbf{N}_{Op} = \frac{\mathbf{b}_p \mathbf{D} v\epsilon}{\left(\frac{\mathbf{D}}{k_f a_p} + \frac{1}{k_p a_p}\right) F} \tag{53}$$

where $\mathbf{b}_f$ and $\mathbf{b}_p$ are coefficients with values usually near unity (Section III, D, 5). These will depend upon $\mathbf{x}$, but frequently are evaluated at $\mathbf{x} = 0.5$.

f. Number of Reaction Units, Column-Capacity Parameter, or Bed-Thickness Modulus, $\mathbf{N}_R$, *or* $\mathbf{s}$. The general treatment of ion-exchange rates is based upon a surface reaction-kinetic driving force which approximates either an external or an internal material-transfer driving force. By

analogy to Hurt's definition of the number of reactor units (H8), a "reaction unit" will be used here as the counterpart of the transfer unit. The number of reaction units (NRU) is given by

$$\mathbf{N}_R\ (= \mathbf{s}) = k_{kin}Qv\rho_b/F \tag{54}$$

where, for adsorption from the gas phase, Q represents q_m. This dimensionless quantity has also been called the column-capacity parameter by Hiester and Vermeulen (H6); it corresponds also to the thickness modulus of Hougen and Marshall (H7). It is related to the "number of theoretical plates," N_o, used by Mayer and Tompkins (M6) and Martin and Synge (M4); usually $\mathbf{N}_R \approx 2N_o$.

Mathematical analysis is needed before $\mathbf{N}_R$ or $\mathbf{N}$ can be related directly to the concentration behavior. The foregoing relations serve primarily to define the height of a transfer (or reaction) unit, H. With $\mathbf{N} = 1$, Eqs. (50) and (51) give

$$H_f = U/k_f a_p \tag{55}$$

$$H_p = \frac{U}{k_p a_p \mathbf{D}} = \frac{d_p{}^2 U}{60 D_p \mathbf{D}} \tag{56}$$

With $\mathbf{N}_R = 1$, Eq. (54) gives

$$H_R = U\epsilon/k_{kin}\rho_b Q \tag{57}$$

The over-all values H_{Of} and H_{Op} can be similarly defined. At $\mathbf{r} = 1$, $H_{Of} = H_{Op} = H_R$. Elsewhere they may differ by a moderate percentage, as will be shown later.

g. Throughput Ratio, $\mathbf{Z}$. This parameter reaches unity when the volume of feed which has passed through the column becomes stoichiometrically equivalent to the adsorption (or exchange) capacity of the column. The stoichiometric volume, V_{stoic}, can be defined by the relation

$$C_o V_{stoic} = q_o{}^* \rho_b v \tag{58}$$

The throughput parameter is then

$$\mathbf{Z} = \frac{V - v\epsilon}{V_{stoic}} = \frac{C_o(V - v\epsilon)}{q_o{}^* \rho_b v} \tag{59}$$

The number of column void-volumes of fluid that have passed through the column, divided by the distribution ratio, also gives the throughput parameter:

$$\mathbf{Z} = (V - v\epsilon)/\mathbf{D}v\epsilon \tag{60}$$

The midpoint of the concentration-history curve ($\mathbf{x} = 0.50$) will usually correspond to a value of $\mathbf{Z}$ near unity.

h. Solution-Capacity Parameter, or Solution Volume (or Time) Modulus,

Θ *or* t. This variable enters into the differential equations as a dimensionless time. However, it can be expressed as the product of **N** (or $\mathbf{N}_R$) and **Z**:

$$\Theta_f = \mathbf{N}_f\mathbf{Z} \tag{61}$$

$$\Theta_p = \mathbf{N}_p\mathbf{Z} \tag{62}$$

$$\mathbf{t} = \mathbf{N}_R\mathbf{Z} \tag{63}$$

Thus the ratio t/s or Θ/Σ used by Hiester and Vermeulen is expressed here by **Z**.

2. *Material Balance*

The conservation equation, for an infinitesimal thickness of bed at any given cross section v, expresses the fact that any loss of component A from the solution flowing through the section must equal the gain of component A on the solid and in the solution at that section:

$$-\left(\frac{\partial c_A}{\partial v}\right)_V = \rho_b\left(\frac{\partial q_A}{\partial \bar{V}}\right)_v + \epsilon\left(\frac{\partial c_A}{\partial \bar{V}}\right)_v \tag{64}$$

It is convenient to consider the volume of saturating solution that has flowed through this cross section, $V - v\epsilon$, as a variable replacing the feed volume, V. By a fundamental property of partial derivatives,

$$\begin{aligned}-\left(\frac{\partial c_A}{\partial v}\right)_V &= \epsilon\left(\frac{\partial c_A}{\partial(\bar{V} - v\epsilon)}\right)_v - \left(\frac{\partial c_A}{\partial v}\right)_{V-v\epsilon} \\ &= \epsilon\left(\frac{\partial c_A}{\partial \bar{V}}\right)_v - \left(\frac{\partial c_A}{\partial v}\right)_{V-v\epsilon}\end{aligned} \tag{65}$$

Hence, Eq. (64) simplifies to

$$-\left(\frac{\partial c_A}{\partial v}\right)_{V-v\epsilon} = \rho_b\left(\frac{\partial q_A}{\partial \bar{V}}\right)_v \tag{66}$$

Introduction of Eqs. (44), (45), and (59) leads to

$$-\left(\frac{\partial \mathbf{x}}{\partial v}\right)_{\mathbf{Z}v} = \left(\frac{\partial \mathbf{y}}{\partial \mathbf{Z}v}\right)_v \tag{67}$$

The NTU or NRU can also be introduced, to give the entirely dimensionless form

$$-\left(\frac{\partial \mathbf{x}}{\partial \bar{\mathbf{N}}}\right)_{\mathbf{ZN}} = \left(\frac{\partial \mathbf{y}}{\partial \mathbf{Z}\bar{\mathbf{N}}}\right)_{\mathbf{N}} \tag{68}$$

It is this *equation of continuity*, rather than the rate equations used with it, that reflects the special behavior of the fixed-bed systems.

B. Limiting Cases of Equilibrium Behavior

1. *Proportionate-Pattern Case (Unfavorable Equilibrium)*

The proportionate-pattern case is a classical one in the theory of chromatography, and was treated by DeVault (D2), Walter (W1), Wilson (W7), and Weiss (W3). It is *assumed* that equilibrium is maintained everywhere in the column, that is, that **N** approaches infinity, due to high mass-transfer rates or to long residence times.

The conservation relation, Eq. (67), is rewritten in the form

$$-\left(\frac{\partial \mathbf{x}}{\partial v}\right)_{\mathbf{Z}v} = \left(\frac{\partial \mathbf{x}}{\partial \mathbf{Z}v}\right)_{v} \frac{d\mathbf{y}}{d\mathbf{x}} \tag{69}$$

Rearrangement gives

$$\frac{d\mathbf{y}}{d\mathbf{x}} = -\frac{(\partial \mathbf{x}/\partial v)_{\mathbf{Z}v}}{(\partial \mathbf{x}/\partial \mathbf{Z}v)_{v}} = \left(\frac{\partial \mathbf{Z}v}{\partial v}\right)_{\mathbf{x}}$$
$$= v\left(\frac{\partial \mathbf{Z}}{\partial v}\right)_{\mathbf{x}} + \mathbf{Z} \tag{70}$$

Following DeVault, this relation can be integrated at constant $\mathbf{x}$ and constant $d\mathbf{y}/d\mathbf{x}$, to give

$$\frac{d\mathbf{y}}{d\mathbf{x}} = \mathbf{Z} + \frac{a}{v} \tag{71}$$

where a is a constant of integration. Equation (71) will be valid only in the range of positive $\mathbf{Z}$ values that gives $0 < \mathbf{x} < 1$. The constant a may be evaluated with the aid of the material-balance integral

$$\int_0^\infty (C_o - c)d(V - v\epsilon) = q_o{}^*\rho_b v \tag{72}$$

or

$$\int_{\mathbf{Z}=0}^{\mathbf{x}=1} (1 - \mathbf{x})d\mathbf{Z} = 1 \tag{73}$$

This relation is comparable to Eq. (66) or (67), but is written for the entire column rather than for a differential section.

For the case of a *constant separation factor*, first treated by Walter (W1), Eq. (23) leads to

$$\frac{d\mathbf{y}}{d\mathbf{x}} = \frac{\mathbf{r}}{[(1 - \mathbf{r})\mathbf{x} + \mathbf{r}]^2} \tag{74}$$

and to $a = 0$. If Eqs. (71) and (74) are combined, there results

$$\mathbf{x} = \frac{(\mathbf{r}/\mathbf{Z})^{1/2} - \mathbf{r}}{1 - \mathbf{r}} \tag{75}$$

The limits of validity are: $\mathbf{x} = 0$ at $\mathbf{Z} = 1/\mathbf{r}$; $\mathbf{x} = 1$ at $\mathbf{Z} = \mathbf{r}$. This is the desired concentration-history equation. It provides a *proportionate pattern*, because $\mathbf{x}$ depends upon $\mathbf{Z}$ only and not upon $\mathbf{N}$ or v. In this case the relative sharpness of the breakthrough curve cannot be increased by lengthening the column.

Where other isotherms apply, the same procedure may be applied; that is, the derivative can be introduced into Eq. (71), and the result introduced into Eq. (73) in order to evaluate a. It is noted that the Freundlich isotherm with $n = 2$, in the form $\mathbf{y} = \mathbf{x}^2$, leads to a breakthrough line of constant slope.

If the equilibrium ceases to be unfavorable, with $\mathbf{r} < 1$, $d\mathbf{x}/d\mathbf{Z}$ will take on a negative slope. As this is prohibited by the material-balance relation, the breakthrough curve for "equilibrium" must be drawn continuously vertical in the concentration region for which $\mathbf{r} \leq 1$.

At $\mathbf{r} \leq 2$, the equilibrium-limit breakthrough given by Eq. (75), is approached only at very high $\mathbf{N}$ values (>500). For $\mathbf{r} \geq 10$, however, this limit will apply at nearly all $\mathbf{N}$ values (≥ 10). The range of validity can only be estimated by comparison with the general result (Section III, D, 1).

2. *Constant-Pattern Case (Favorable Equilibrium)*

It will next be *assumed* that a region of $\mathbf{r}$ values exists where the effluent concentration pattern is independent of column length (instead of proportional to it). This is equivalent to $(\partial \mathbf{Z}v/\partial v)_{\mathbf{x}}$ constant; the difference of V values for two different values of $\mathbf{x}$ (e.g., $\mathbf{x} = 0.05$ and $\mathbf{x} = 0.95$) remains constant regardless of the length of the column.

With this assumption, Eq. (70) again applies, and its integration gives

$$\mathbf{y} = (\text{const.})\ \mathbf{x} \tag{76}$$

Since $\mathbf{y}$ and $\mathbf{x}$ have the same limits,

$$\mathbf{y} = \mathbf{x} \tag{77}$$

This relation becomes the continuity condition for the constant-pattern case.

In order to obtain realistic concentration-history curves, the rate can no longer be assumed infinite. Instead, the breakthrough becomes dependent upon rate. Since $V_{0.95} - V_{0.05}$ is independent of v, it follows that $\mathbf{Z}_{0.95} - \mathbf{Z}_{0.05}$ is inversely proportional to v. Thus, in agreement with the results of the previous section, the breakthrough curves are relatively steeper at higher v or higher $\mathbf{N}$.

The constant-pattern case was first identified and discussed by Bohart and Adams (B6), Wicke (W5), and Sillén (S4). Michaels termed

it the "constant exchange zone" case (M7), while Dryden (D6) has called it the "constant pattern."

a. External Diffusion. For irreversible adsorption ($\mathbf{r} = 0$), Eqs. (31) and (48) lead to

$$d\mathbf{x}/d\tau = k_f a_p \mathbf{D}\mathbf{x} \tag{78}$$

Integration for a column of given v, with evaluation of the constant by Eq. (73), and substitution of Eqs. (50) and (59), gives the result of Drew, Spooner, and Douglas (D5), which has been applied also by Selke and Bliss (S2),

$$1 + \ln \mathbf{x} = k_f a_p \mathbf{D}(V - v\epsilon - V_{stoic})/F$$

or

$$\ln \mathbf{x} = \mathbf{N}_f(\mathbf{Z} - 1) - 1 \tag{79}$$

Equation (79) applies between $\mathbf{Z} = 1/\mathbf{N}_f$ (below which $\ln \mathbf{x} = -\mathbf{N}_f$) and $\mathbf{Z} = 1 + 1/\mathbf{N}_f$, at which $\mathbf{x}$ becomes unity. Figure 7 shows a breakthrough curve calculated from Eq. (79) for $\mathbf{N}_f = 4$.

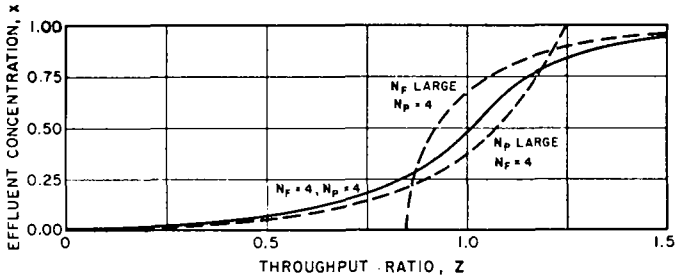

FIG. 7. Breakthrough curves under irreversible conditions, for fluid-phase, particle-phase, and combined resistances controlling. Courtesy of *Industrial and Engineering Chemistry.*

This method is applicable to partially reversible adsorption ($0 < \mathbf{r} < 1$), for which $\mathbf{x}^*$ must be replaced by a function of $\mathbf{y}$ (hence, $\mathbf{x}$) that is evaluated from the appropriate isotherm. A graphical method has been developed by Eagleton and Bliss (E1, T4) which can be used when the analytical relations become unmanageable.

Michaels (M7) has solved Eq. (31) for the case of a *constant separation factor.* His result is

$$\frac{1}{1 - \mathbf{r}} \ln \frac{\mathbf{x}_2(1 - \mathbf{x}_1)}{\mathbf{x}_1(1 - \mathbf{x}_2)} + \ln \frac{1 - \mathbf{x}_2}{1 - \mathbf{x}_1} = \mathbf{N}_f(\mathbf{Z}_2 - \mathbf{Z}_1) \tag{80}$$

If this relation were extended to a value of $\mathbf{r} = 1$, the rate expressed as $d\mathbf{y}/d\tau$ would fall to zero for all finite values of $\mathbf{N}_f$. Again, the range of

validity must be established by comparison with a general solution (Section III, D, 1). The following limits are found:

r	0	0.2	0.5	0.8
Minimum N	(4)	10	25	75

b. Internal Solid-Phase Diffusion. An exact solution for the *irreversible* constant-pattern breakthrough has been provided by Wicke (W5), Boyd *et al.* (B8), and others:

$$\mathbf{x} = 1 - \frac{6}{\pi^2} \sum_{n=1}^{\infty} \frac{1}{n^2} e^{-n^2[\psi \mathbf{N}_p(\mathbf{Z}-1)+0.97]} \tag{81}$$

As in Eq. (51), $\mathbf{N}_p = 60D_p\mathbf{D}v\epsilon/Fd_p^2$. For this case ($\mathbf{r} = 0$), $\psi = 4\pi^2/60$. Glueckauf and Coates (G5) have provided the linear-driving-force approximation of Eq. (37), which in the irreversible case becomes

$$\frac{d\mathbf{x}}{d\tau} = \frac{60D_p}{d_p^2}\mathbf{D}(1 - \mathbf{x}) \tag{82}$$

which integrates to

$$\mathbf{x} = 1 - e^{-[\mathbf{N}_p(\mathbf{Z}-1)+1]} \tag{83}$$

If used in this form, Eq. (83) gives a good fit to Eq. (81) in the lower part of the curve, when $0 < \mathbf{x} < 0.6$. However, the slopes in the asymptotic, high-concentration region will be high by a factor of $15/\pi^2$. If conversely a match is made in the high-concentration region, a moderately large error results in the lower part of the curve.

For a partially irreversible adsorption, i.e. one with highly favorable equilibrium, and with a *constant separation factor*, Glueckauf and Coates's result becomes:

$$\frac{\mathbf{r}}{1-\mathbf{r}} \ln \frac{\mathbf{x}_2(1-\mathbf{x}_1)}{\mathbf{x}_1(1-\mathbf{x}_2)} + \ln \frac{1-\mathbf{x}_1}{1-\mathbf{x}_2} = \mathbf{N}_p(\mathbf{Z}_2 - \mathbf{Z}_1) \tag{84}$$

The limits of validity here are the same as listed above for Eq. (80).

A quadratic-driving-force approximation has been developed by Vermeulen (V3). For $\mathbf{r} = 0$ this fits Eq. (81) closely over the entire range of $\mathbf{x}$. This can be extended to the general form:

$$\frac{d\mathbf{y}}{d\tau} = \frac{60\psi D_p}{d_p^2} \cdot \frac{(\mathbf{y}^*)^2 - \mathbf{y}^2}{2(\mathbf{y} - \mathbf{y}_o)} \tag{85}$$

From Glueckauf's recent work (G3), the author finds

$$\psi = \frac{\pi^2}{\pi^2\mathbf{r} + 15(1-\mathbf{r})} \tag{86}$$

For the completely irreversible case, Eq. (85) integrates to

$$\mathbf{x} = [1 - e^{-\psi[\mathbf{N}_p(Z-1)+0.93]}]^{1/2} \tag{87}$$

This result has been used for extrapolation at $\mathbf{r} = 0$ into the region of $\mathbf{N}_p$ values below 4, where $\mathbf{y}$ obeys Eq. (81) or (87) with an exponential term $e^{-\mathbf{N}_p(Z-Z_b)}$ for which $\mathbf{N}_p\mathbf{Z}_b$ $(= \Theta_b)$ is a known function of $\mathbf{N}_p$ (V3). In this region $\mathbf{x}$ no longer exhibits a constant pattern. The resulting curves for $\mathbf{x}$ give a much improved fit to data of Vermeulen and Huffman (V6) and Dryden (D6). The relative simplicity of Eq. (87), combined with good accuracy, should make it a useful replacement for Eq. (81) in many areas of application.

Fujita (F2) has solved the linear-driving-force case for adsorption of two solutes in the "irreversible" region. His treatment assumes that the two solutes have different rate coefficients, and that the equilibrium constant between them is not unity. The results generally are not obtained in closed form, but Fujita's article gives plots of the results for several typical cases.

c. Pore Diffusion. This problem has been solved for the irreversible case ($\mathbf{r} = 0$), in unpublished work by Acrivos and Vermeulen. The fluid-phase concentration in the pores is assumed negligible compared to the solid-phase value. Equation (32) then becomes

$$\frac{D_{pore}}{r^2}\frac{\partial}{\partial r}\left(r^2\frac{\partial c_i}{\partial r}\right) = \rho_b\frac{\partial q_i}{\partial \tau} \tag{88}$$

Differentiation of Eq. (33) gives

$$\frac{\partial}{\partial r}\left(\frac{dq}{d\tau}\right) = \frac{3r^2}{r_p{}^3}\frac{\partial q_i}{\partial \tau} \tag{89}$$

Combination of Eqs. (88) and (89) gives

$$\frac{dq}{d\tau} = \frac{3D_{pore}r^2}{\rho_b r_p{}^3}\frac{\partial c_i}{\partial r} \tag{90}$$

In the irreversible case, the concentration wave entering the particle will saturate each spherical layer before it penetrates further. That is, c_i cannot exceed zero at a particular radius $r = r_i$ until q_i at that r has become equal to the saturation value q_m. With $c/C_o = q/q_m = 1 - (r_i/r_p)^3$ by material balance over one particle, Eq. (90) leads to

$$\frac{dr_i}{d\tau} = -\frac{k_{pore}}{15}\frac{r_p{}^2 + r_p r_i + r_i{}^2}{r_i} \tag{91}$$

where

$$k_{pore} = \frac{60D_{pore}C_o}{\rho_b q_m d_p{}^2} \tag{92}$$

Integration of Eq. (91) can be followed by numerical evaluation of $\mathbf{x}$. The result fits the empirical relation

$$\mathbf{x} = 0.557[\mathbf{N}_{\text{pore}}(\mathbf{Z} - 1) + 1.15] - 0.0774[\mathbf{N}_{\text{pore}}(\mathbf{Z} - 1) + 1.15]^2 \quad (93)$$

with $\mathbf{N}_{\text{pore}} = 60D_{\text{pore}}v/Fd_p^2$. Whereas (at $\mathbf{r} = 0$ only) the external-diffusion curve has a finite limit at $\mathbf{x} = 1$, and the solid-phase internal-diffusion curve has a finite limit at $\mathbf{x} = 0$, the pore-diffusion curve has two such limits; at $\mathbf{x} = 0$, $\mathbf{Z} = 1 - (1.15/\mathbf{N}_{\text{pore}})$, and at $\mathbf{x} = 1$, $\mathbf{Z} = 1 + (2.43/\mathbf{N}_{\text{pore}})$.

d. Combined External- and Internal-Diffusion Resistances. Where these two mechanisms have similar rates, external diffusion will tend to predominate at low extents of breakthrough and internal diffusion will have more of a retarding effect as full saturation is approached. The rates given by Eqs. (31) and (85) can be set equal, in terms of interface concentrations that are in mutual equilibrium:

$$k_f(\mathbf{x} - \mathbf{x}_i) = k_p\mathbf{D}\psi \frac{\mathbf{y}_i^2 - \mathbf{x}^2}{2\mathbf{x}} \quad (94)$$

In the initial stages of breakthrough, under *irreversible* conditions, $\mathbf{x}_i = 0$ and $\mathbf{y}_i < 1$, so that breakthrough follows the external-diffusion curve (Eq. 79). Eventually $\mathbf{y}_i$ reaches unity, and abruptly $\mathbf{x}_i$ becomes finite; Eq. (87) then applies. Equation (94) can be solved for $\mathbf{x}$ at this transition point. The integration constants in Eqs. (79) and (87) must be modified by introducing Eq. (73), as described elsewhere by the author (V3). The curve resulting from $\mathbf{N}_f = 4$ and $\mathbf{N}_p = 4$ is shown in Fig. 7.

For partially reversible conditions, evaluation of $\mathbf{x}_i$ and $\mathbf{y}_i$ is more difficult. The method of Section III, D, 6 is applicable.

e. Surface Reaction-Kinetics Controlling. This empirical case is useful, at $\mathbf{r}$ values between zero and 0.5, for treatment of the combined-mechanism region and of pore diffusion, or for preliminary interpretation of data when the mechanism is not known. Equations (35) and (77) give

$$\frac{d\mathbf{x}}{d\mathbf{Z}} = \mathbf{N}_R(1 - \mathbf{r})\mathbf{x}(1 - \mathbf{x}) \quad (95)$$

Integration gives

$$\frac{1}{1 - \mathbf{r}} \ln \frac{\mathbf{x}}{1 - \mathbf{x}} = \mathbf{N}_R(\mathbf{Z} - 1) \quad (96)$$

This result was derived by Walter (W1) and Sillén (S4), and much earlier in the case of $\mathbf{r} = 0$ by Bohart and Adams (B6). Like the combined-mechanism curve of Fig. 7, Eq. (96) gives breakthrough curves which are asymptotic at $\mathbf{x}$ values of both zero and unity.

f. Application to Mixed-Bed Deionization. The removal of a salt M^+X^- from water in a single bed utilizes the three reactions:

$$\begin{aligned} HCat + M^+ &= MCat + H^+ \\ AnOH + X^- &= AnX + OH^- \\ H^+ + OH^- &= H_2O \end{aligned}$$

where Cat represents cationic resin, and An, anionic resin. As in simple adsorption, but unlike ordinary ion exchange, the total ionic concentration of the effluent has a very small value. In this region of concentrations, external diffusion is likely to control.

The adsorption is irreversible ($\mathbf{r} = 0$) because of the neutralization reaction. Sharp breakthrough curves are obtained, and thus high flow rates are possible (K7, C1).

An idealized limiting situation can be considered, where the two resins are present in stoichiometric proportions. Then

$$(Q\rho_b v)_{HCat} = (Q\rho_b v)_{AnOH} = C_o(V - v_T\epsilon)/Z \tag{97}$$

with the total bed volume $v_T = v_{HCat} + v_{AnOH}$. Equation (79) can then be applied to calculate the breakthrough curve.

C. Column Dynamics under Linear Equilibrium

1. *General Result*

Linear equilibrium involves constant-separation-factor conditions, with the value of the factor $\mathbf{r}$ equal to unity. In binary ion exchange involving only one component in the feed, $\mathbf{r} = 1$ corresponds to $K = 1$, a condition which may be approached but seldom is realized exactly. In ion exchange with a mixed feed, $\mathbf{r}$ tends toward unity as the feed mole-fraction of the exchanging component $[(c_A)_o/C_o]$ diminishes (Section III, D, 1b). For simple adsorption, $\mathbf{r} = 1/(1 + K_L p_o)$ by Eq. (18), and the case of $\mathbf{r} = 1$ corresponds to a wide range of weak adsorption where $K_L p_o \ll 1$ as has been noted by Wicke (W5), Thomas (T1), and Hougen and Marshall (H7).

When $\mathbf{r} = 1$, the same form of equation is obtained from several different rate-determining mechanisms. For external diffusion, Eq. (31) becomes

$$\left(\frac{\partial \mathbf{y}}{\partial \tau}\right)_{\mathbf{N}} = \frac{k_f a_p(\mathbf{x} - \mathbf{y})}{\mathbf{D}} \tag{98}$$

For internal diffusion, Eq. (37) or (85) gives approximately

$$\left(\frac{\partial \mathbf{y}}{\partial \tau}\right)_{\mathbf{N}} = k_p a_p(\mathbf{x} - \mathbf{y}) \tag{99}$$

By analogy to Eqs. (98) and (99), the pore-diffusion relation is approximately

$$\left(\frac{\partial \mathbf{y}}{\partial \tau}\right)_{\mathbf{N}} = k_{\text{pore}}(\mathbf{x} - \mathbf{y}) \tag{100}$$

The surface-reaction expression, from Eq. (35), is

$$\left(\frac{\partial \mathbf{y}}{\partial \tau}\right)_{\mathbf{N}} = k_i C_o(\mathbf{x} - \mathbf{y}) \tag{101}$$

In each case, then,

$$\left(\frac{\partial \mathbf{y}}{\partial \mathbf{ZN}}\right)_{\mathbf{N}} = \mathbf{x} - \mathbf{y} \tag{102}$$

Integration of Eqs. (102) and (68), jointly, has been carried out by Anzelius (A3) and Schumann (S1). The results can be expressed as

$$\mathbf{x} = \mathbf{J}(\mathbf{N},\mathbf{ZN}) \tag{103}$$

$$\mathbf{y} = 1 - \mathbf{J}(\mathbf{ZN},\mathbf{N}) \tag{104}$$

where the function $\mathbf{J}$ of two variables s and t is given by

$$\mathbf{J}(s,t) = 1 - \int_0^s e^{-t-\xi} I_o(2\sqrt{t\xi}) d\xi \tag{105}$$

and I_o is a modified Bessel function of the first kind. $\mathbf{J}(s,t)$ is related to Thomas's function $\phi(s,t)$ in the following manner (T1)

$$\mathbf{J}(s,t) = 1 - e^{-s-t}\phi(s,t) \tag{106}$$

It is also related to Brinkley's function g, of which a punched-card table is available (B10):

$$\mathbf{J}(s,t) = 1 - g(\sqrt{s},\sqrt{t}) \tag{107}$$

Another relation useful in the evaluation of $\mathbf{J}$ is

$$1 - \mathbf{J}(s,t) = \mathbf{J}(t,s) - e^{-t-s} I_o(2\sqrt{st}) \tag{108}$$

Since $I_o(0) = 1$ it is apparent that the lower boundaries of $\mathbf{J}(s,t)$ are

$$\mathbf{J}(0,t) = 1; \qquad \mathbf{J}(s,0) = e^{-s}$$

It can also be shown that the upper limits of $\mathbf{J}$ are:

$$\lim_{s \to \infty} \mathbf{J}(s,t) = 0; \qquad \lim_{t \to \infty} \mathbf{J}(s,t) = 1$$

In the region where the variables of the argument are both greater than 10, use has been made of an asymptotic expansion due to Onsager and given by Thomas (T2) which reduces to:

$$\mathbf{J}(s,t) = \frac{1}{2}\left\{1 + \operatorname{erf}(\sqrt{t} - \sqrt{s}) + \frac{e^{-(\sqrt{s}-\sqrt{t})^2}}{\pi[\sqrt{t} + \sqrt[4]{st}]}\right\} \tag{109}$$

accurate to within 1% when $\sqrt{st} \geq 6$, where (for any number z)

$$\text{erf}\,(z) = \frac{2}{\sqrt{\pi}} \int_0^z e^{-\eta^2} d\eta \tag{110}$$

as given in standard tables. At $\sqrt{st} \geq 60$, the last term of Eq. (109) can be dropped.

Figure 8, on logarithmic-probability coordinates, shows the behavior of the **J** function. The concentration histories, as plotted against time on

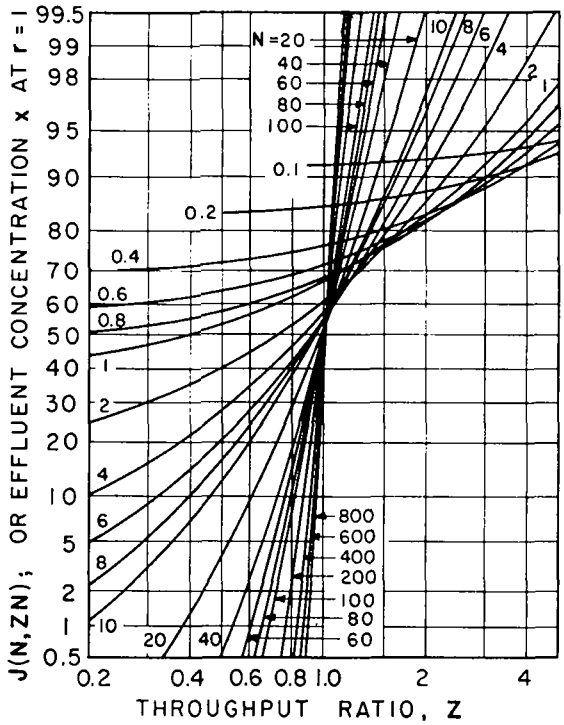

FIG. 8. Dependence of the J function upon NTU and throughput ratio. Courtesy of *Chemical Engineering Progress* (H6).

linear scales, normally are S-shaped. The probability scale for **x** largely eliminates the curvature of such plots and also makes it possible to plot accurately those values that are either very small or very near to unity. The logarithmic scale for **Z** makes it possible to compare experimental **x**-time plots directly with the theoretical curves; this curve-fitting technique was utilized in analogous heat-transfer calculations by Furnas (F3), and in ion exchange work by Beaton and Furnas (B5).

The **J** function is also given by Hougen and Marshall (H7) on logarithmic coordinates, by Furnas (F3) on linear coordinates, and by Klinkenberg (K3) in nomographic form. Goldstein (G6) and Klinkenberg have analyzed the behavior of the **J** function under various limiting conditions.

2. *External and Internal Diffusion in Series*

At $\mathbf{r} = 1$, for combinations of Eqs. (98) and (99), or (98) and (100), the transfer resistances can be added; for instance,

$$\frac{1}{k_{\text{kin}}C_o} = \frac{\mathbf{D}}{k_f a_p} + \frac{1}{k_p a_p} \tag{111}$$

and the mathematical results are still expressed by Eqs. (103) and (104). However, Eqs. (99) and (100) do not give precise results at **N** values below 50.

The exact integration of Eq. (32) or (36) under linear-equilibrium conditions, in conjunction with Eqs. (1) and (68), has been carried out by Rosen (R1) and by Kasten *et al.* (K1). Rosen's computed results have been presented in graphical and tabular form. His variables have the following correspondence to the ones used here: $x = \mathbf{N}_p/5$; $y/x = 2\mathbf{Z}/3$; $x/\nu = \mathbf{N}_f$.

Rosen, and also Wicke (W5), have given an asymptotic relation for solid-phase diffusion or for pore diffusion, at $\mathbf{r} = 1$, which can be expressed as

$$\mathbf{x} = \tfrac{1}{2}[1 + \text{erf } \tfrac{1}{2}\sqrt{\mathbf{N}}\,(\mathbf{Z} - 1)] \tag{112}$$

Equation (109) gives for the same cases

$$\mathbf{x} = \tfrac{1}{2}[1 + \text{erf } \sqrt{\mathbf{N}}\,(\sqrt{\mathbf{Z}} - 1)] \tag{112a}$$

If **Z** is near unity, these two expressions are numerically equivalent.

3. *Longitudinal Dispersion*

The effect of longitudinal dispersion in a column, as a factor which reduces the sharpness of breakthrough curves, has been considered by Barrow and co-workers (B3), Ledoux (L4), and others. Wicke (W5) has discussed the combined effect of longitudinal dispersion with internal diffusion, while Lapidus and Amundson (L3) have reviewed the combined effect with external diffusion. Van Deemter *et al.* (V2) have recently studied this problem with respect to gas chromatography.

For the case where fluid-particle equilibrium is closely approached, and the breakthrough slope is determined entirely by longitudinal

dispersion, the foregoing authors (L3, W5) give a result equivalent to:

$$\mathbf{x} = \frac{1}{2}\left[1 + \operatorname{erf}\left\{\frac{1}{2}\sqrt{\frac{Uv^2\epsilon}{ESV}}\,\frac{V - V_{\text{stoic}} - v\epsilon}{v\epsilon}\right\}\right] \tag{113}$$

where E is the effective dispersivity, cm.^{2}/sec. In order to avoid an indeterminate error-function argument when V_{stoic} vanishes, it is convenient to define a modified throughput ratio, $\mathbf{z}$:

$$\mathbf{z} = \frac{V}{V_{\text{stoic}} + v\epsilon} \tag{113a}$$

This function satisfies the relation $\mathbf{D}(\mathbf{Z} - 1) = (\mathbf{D} + 1)(\mathbf{z} - 1)$; hence, for large $\mathbf{D}$, $\mathbf{z} \approx \mathbf{Z}$. An effective number of transfer units for longitudinal dispersion is defined by

$$\mathbf{n} = (\mathbf{D} + 1)Uv/SE \tag{113b}$$

Equation (113) then becomes

$$\mathbf{x} = \tfrac{1}{2}[1 + \operatorname{erf} \tfrac{1}{2}\sqrt{\mathbf{n}}\,(\mathbf{z} - 1)] \tag{113c}$$

which is seen to have the same form as Eq. (112). In the absence of channeling, and with the eddy dispersivity large relative to the molecular diffusivity of the fluid, the value of eddy dispersivity determined for gas flow in catalyst beds can be used to estimate $\mathbf{n}$. Since the eddy dispersivity is near $2d_p\epsilon U$, for laminar flow (J1), often $\mathbf{n} \approx (\mathbf{D} + 1)v/2d_p\epsilon S$. The height of one effective transfer unit is then $H_D \approx 2d_p\epsilon/(\mathbf{D} + 1)$.

Calculations of this type are particularly applicable to the flushing or rinsing of ion exchange columns with distilled water. In this case, $\mathbf{D} = 0$. For beds with $\mathbf{D} = 0$ and $\mathbf{n} < 20$, Jacques and Vermeulen (J1) have found that Einstein's random-walk approach (E2) gives a result which is intermediate to the diffusion equation (A4, M8) and the Poisson distribution (K6), and is thus most apt to apply to actual packed-bed conditions:[4]

$$\mathbf{x} = 1 - \mathbf{J}(\mathbf{nz}, \mathbf{n}) \tag{113d}$$

This reduces to Eq. (113c) at large values of $\mathbf{n}$.

[4] For use in interpreting infinitesimal pulse-function distributions, or chromatograms (cf. Section IV, C, 2), with longitudinal dispersion controlling, differentiation of Eq. (113d) yields

$$\mathbf{x} \propto e^{-\mathbf{n}-\mathbf{nz}} I_0(2\mathbf{n}\sqrt{\mathbf{z}}) \tag{113e}$$

At large $\mathbf{n}$, this becomes

$$\ln \mathbf{x} = \ln \mathbf{x}_{\max} - \tfrac{1}{4}\mathbf{n}(\mathbf{z} - 1)^2 \tag{113f}$$

which has the same form as Eq. (166).

4. *Analogous Treatment of Heat Transfer*

Under conditions of constant heat capacities for the solid checkerwork of a heat regenerator, and for the fluid phases releasing or withdrawing thermal energy, this problem can be solved as a linear-equilibrium case. The relative temperatures are

$$\mathbf{x} = \frac{T_f - T_o}{T_\infty - T_o}; \qquad \mathbf{y} = \frac{T_p - T_o}{T_\infty - T_o} \tag{114}$$

where T_o is the initial temperature of the bed, T_∞ the temperature it will reach at saturation, T_f the instantaneous temperature of the fluid, and T_p the instantaneous average temperature of the solid.

The controlling resistance may be taken as external to the particle:

$$\frac{\partial \mathbf{y}}{\partial \tau} = \frac{k_H a_p \epsilon}{c_p} (\mathbf{x} - \mathbf{y}) \tag{115}$$

where k_H is the heat-transfer coefficient, and c_p is the heat capacity of the solid per unit packed volume. Also, c_f is the heat capacity per unit volume of the fluid, in the following relations:

$$\mathbf{D}_H = c_p/c_f\epsilon \tag{116}$$

$$\mathbf{N}_{Hf} = \frac{k_H a_p}{c_f} \frac{v\epsilon}{F} \tag{117}$$

$$\mathbf{Z}_H = \frac{c_f}{c_p} \frac{V - v\epsilon}{v} \tag{118}$$

$\mathbf{N}_H$ represents the number of heat-transfer units.

If, instead, the conductance of the particle is limiting, it is true approximately that

$$\frac{d\mathbf{y}}{dt} = \frac{60 D_H}{d_p^2} (\mathbf{x} - \mathbf{y}) \tag{119}$$

where D_H is the thermal diffusivity of the solid. Here

$$\mathbf{N}_{Hp} = \frac{60 D_H}{d_p^2} \frac{v\epsilon}{F}$$

and $\mathbf{Z}_H$ and $\mathbf{D}_H$ are unchanged.

In either of the above cases, the relative temperatures are given by Eq. (103) or (113) (or Fig. 8) for the effluent, and by Eq. (104) for the checkerwork. Rosen's numerical solutions (R1) can also be applied directly, if solid-phase conduction accounts for part (or all) of the transfer resistance.

5. *Use of Curves to Predict Breakthrough Behavior*

For a column of given height or volume, the smaller of the calculated $\mathbf{N}$ values will control unless the values are of the same magnitude. If the

column dimensions, the flow rate, and the cycle period are all specified, the dimensionless parameters **N** and **Z** can be calculated, and (if **r** = 1) **x** can be read from Fig. 8. For example, assume that $k_f a_p$ is known to be 20 min.$^{-1}$; $\epsilon = 0.4$; $\rho_b = 0.5$ gm./ml.; and $q_o^* = 50$ mg./gm. In addition, design values are specified for $v = 75$ ml., $C_o = 0.5$ mg./ml., and $F = 30$ ml./min. It follows that **D** = 125 by Eq. (48), and $\mathbf{N}_t = 20$ by Eq. (50). The effluent time ($\tau - v\epsilon/F$), corresponding to **Z** = 1, is indicated by Eq. (59) to be $\mathbf{D}v\epsilon/F$ or 125 min. If it is desired to calculate **x** at a time ($\tau - v\epsilon/F$) = 75 min., the coordinates **Z** = 0.60 and **N** = 20 in Fig. 8, show that **x** = 0.10.

If the breakthrough value is specified along with **N**, the chart can be used to find **Z**. If **x** and τ are specified and the height of the column is to be determined, a trial-and-error solution must be made on Fig. 8; or the value of **N** can be read off a plot of **x** against **NZ**, since here $\mathbf{NZ} \approx (k_f a_p/\mathbf{D})$.

6. *Radial Beds*

The use of annular cylindrical beds, fed through a central channel and drained at the periphery, is of potential interest in cases where high throughput rates and wide but shallow beds are desired. Radial-flow geometry is also characteristic of one operating method used in paper chromatography.

Lapidus and Amundson (L2) have solved this problem for a constant volumetric flow rate. For **r** = 1, the result is again given by Eq. (103).[5] The dimensionless parameters have their usual values, with v calculated as

$$v = \pi l(R_e^2 - R_i^2) \tag{120}$$

where l is the axial depth of the bed; R_e is the exterior radius; and R_i is the interior radius. In this case the external mass-transfer coefficient k_f, being a function of the linear velocity, will vary with the radius.

The derivations for radial beds include the general reaction-kinetic case with constant separation factor, analogous to the treatment of axial-flow beds in the next section. An equation identical in form with Eq. (121) is obtained by Lapidus and Amundson.

D. Column Dynamics at a Constant Separation Factor

1. *The Method of Surface Reaction Kinetics*

a. Thomas's Solution. The most general relation that has been developed for breakthrough behavior is that of H. C. Thomas (T1), which

[5] The two terms in the argument of **J** are inverted in the reference (L2) and in the dissertation of Hiester (H1), relative to Eq. (103).

includes the equilibrium parameter **r** as an independent variable along with the number of transfer units **N** and the throughput ratio **Z**. Equations (35) and (68) have been solved, to give

$$\mathbf{x} = \frac{\mathbf{J}(\mathbf{rN}_R,\mathbf{ZN}_R)}{\mathbf{J}(\mathbf{rN}_R,\mathbf{ZN}_R) + e^{(\mathbf{r}-1)\mathbf{N}_R(\mathbf{Z}-1)}[1 - \mathbf{J}(\mathbf{N}_R,\mathbf{rZN}_R)]} \tag{121}$$

and a similar relation (cf. Eq. 156) for **y**. An extensive graphical representation of **x** has been given by Hiester and Vermeulen (H6), and numerical values have been computed and tabulated by Opler and Hiester (O1).

It is apparent that Eq. (121) contains the **J** function as a limiting case, at $\mathbf{r} = 1$. This equation also has been shown to reduce to the constant-pattern result (Eq. 96) with $\mathbf{r} \ll 1$, and to the proportionate-pattern result (Eq. 75) with $\mathbf{r} \gg 1$, in work by Hiester and Vermeulen (H6) and Gilliland and Baddour (G2). Goldstein (G6) has reviewed this result from a mathematical viewpoint, and has presented limiting forms which give an accurate approximation in certain regions; his variables u, s, and y correspond respectively to the present **x**, **N**, and **ZN**.

In the writer's view, the Thomas equation is the most important single result in the entire theory of adsorption-column performance. By reference to this result, all other solutions are found to be classifiable in terms of their **r** and **N** values.

b. Generalized Behavior of Binary Systems. Thomas's result has been applied mainly to two-component exchange-adsorption systems in which a fluid containing one component interacts with a solid phase containing initially only the other component; or to one-component adsorption involving solid that initially is entirely free of adsorbed material. However, Thomas (T2) has also shown that elution from a completely saturated bed and saturation of a completely eluted bed are complementary processes, each of which has an equilibrium constant that is the reciprocal of the constant for the other. Amundson (A2) has extended Thomas's methods to obtain an algebraic framework for numerical integration of the binary case in which the initial solid-phase composition varies with position in the column, and the feed composition varies with time (but also under the restriction of constant total flow rate).[6]

The problem to be considered now is one of exchange adsorption with *uniform partial presaturation* (V5). The initial solid-phase and entering fluid-phase concentrations are each to be uniform (independent of position or time, respectively), but may each involve any desired proportion of each of the two components A and B.

In a column that is uniformly presaturated with component A to any

[6] On p. 819 of reference A2, the definitions of parameters $F'(x)$ and $G'(y)$ have been interchanged.

specified level (for example, by mixing A-resin and B-resin; or by saturating completely with a solution containing both A and B ions), the initial concentration $(q_A)_o$ corresponds to an equilibrium concentration $(c_A)_o^*$ in the solution phase at a given total solution concentration C_o. With a feed at $(c_A)_o$, only the amount $[(c_A)_o - (c_A)_o^*]$ will be removed from each unit volume of solution under the most favorable conditions. Likewise, if $(q_A)_o^*$ is the resin concentration that would be in equilibrium with feed solution at $(c_A)_o$, the resin at most will accumulate only $[(q_A)_o^* - (q_A)_o]$ moles of A per unit weight. The equilibrium is given by Eq. (21), with $\mathbf{x}$ replacing N.

In order to utilize the saturation functions derived for pure feed and pure resin, a solution saturation-fraction must be defined,

$$\lambda = \frac{c_A - (c_A)_o^*}{(c_A)_o - (c_A)_o^*} = \frac{\mathbf{x} - \mathbf{x}_o^*}{\mathbf{x}_o - \mathbf{x}_o^*} \tag{122}$$

and a resin saturation-fraction,

$$\omega = \frac{q_A - (q_A)_o}{(q_A)_o^* - (q_A)_o} = \frac{\mathbf{y} - \mathbf{y}_o}{\mathbf{y}_o^* - \mathbf{y}_o} \tag{123}$$

where

$$\mathbf{x}_o = (c_A)_o/C_o, \qquad \mathbf{x}_o^* = (c_A)_o^*/C_o$$
$$\mathbf{y}_o = (q_A)_o/Q, \qquad \mathbf{y}_o^* = (q_A)_o^*/Q$$

The numerical solutions for $\lambda = \lambda(\mathbf{r},\mathbf{N},\mathbf{Z})$ and $\omega = \omega(\mathbf{r},\mathbf{N},\mathbf{Z})$ will correspond exactly to those derived for $\mathbf{x}$ and $\mathbf{y}$, if the parameters can be redefined so that λ and ω, respectively, will replace $\mathbf{x}$ and $\mathbf{y}$ in the rate and material-balance relations (Eqs. 68 and 35) to give:

$$\left(\frac{\partial\omega}{\partial \mathbf{Z}\mathbf{N}_R}\right)_{\mathbf{N}_R} = \lambda(1-\omega) - \mathbf{r}\omega(1-\lambda) = -\left(\frac{\partial\lambda}{\partial \mathbf{N}_R}\right)_{\mathbf{Z}\mathbf{N}} \tag{124}$$

This leads to the relations:

$$\mathbf{r} = \frac{(K^{II}-1)\mathbf{x}_o^* + 1}{(K^{II}-1)\mathbf{x}_o + 1} \tag{125}$$

$$\mathbf{N}_R = \frac{kQ\rho_b}{(K^{II}-1)\mathbf{x}_o^* + 1}\frac{v}{F} \tag{126}$$

and

$$\mathbf{Z} = \frac{[(K^{II}-1)\mathbf{x}_o + 1][(K^{II}-1)\mathbf{x}_o^* + 1]}{\mathbf{D}K^{II}}\frac{V - v\epsilon}{v\epsilon} \tag{127}$$

To use this method for simple adsorption (instead of exchange

adsorption), the equations become

$$\mathbf{r} = \frac{1 + K_L p_o^*}{1 + K_L p_o} \tag{128}$$

$$\mathbf{N}_R = \frac{kQ\rho_b}{1 + K_L p_o^*} \frac{v}{F} \tag{129}$$

and

$$\mathbf{Z} = \frac{(1 + K_L p_o)(1 + K_L p_o^*)}{\mathbf{D} K_L p_o} \frac{V - v\epsilon}{v} \tag{130}$$

The theory for partially presaturated columns serves to unify the calculation methods for exchange adsorption and Langmuir adsorption, by including within its framework several situations which previously have had to be solved as isolated problems. These situations are those of elution of a completely saturated column, and of saturation and chromatography of trace components (the trace linear-equilibrium situation).

c. Elution from a Completely Saturated Column. In saturation, $\mathbf{x}_o = 1$ and $\mathbf{x}_o^* = 0$. In elution of the same component, by means of desorption or of the reverse exchange, $\mathbf{x}_o^\dagger = 0$ and $(\mathbf{x}_o^\dagger)^* = 1$, where the dagger (†) designates the parameters for the elution cycle. From Eqs. (122–130), with the unlabeled parameters indicating the saturation cycle, it can be shown (V5) that

$$\lambda^\dagger = \mathbf{x}^\dagger = 1 - \mathbf{x} \tag{131}$$

$$\omega^\dagger = \mathbf{y}^\dagger = 1 - \mathbf{y} \tag{132}$$

$$\mathbf{r}^\dagger = 1/\mathbf{r} \tag{133}$$

$$\mathbf{N}_R{}^\dagger = \mathbf{r}\mathbf{N}_R \tag{134}$$

$$\mathbf{Z}^\dagger = \mathbf{Z} \tag{135}$$

These results are well known from Thomas's work (T2), but serve to confirm the correctness of the uniform-partial-presaturation theory.

d. Behavior of Trace Components. The binary trace situation represents a linear equilibrium, because of the small extent of saturation of the adsorbent by a trace component, A. For ion exchange, with $c_A \ll C_o$, it follows that $C_o = c_A + c_G \approx c_G$, where c_G is the concentration of the gross or carrier ion. For adsorption, $K_L p_o \ll 1$. In both processes, generally $\mathbf{x}_o^* = 0$, although this limitation is not a necessary one. From Eq. (125) or (128),

$$\mathbf{r} = \frac{C_o}{(K^{II} - 1)(c_A)_o + C_o} \text{ or } \frac{1}{1 + K_L p_o} \approx 1 \tag{136}$$

A trace component can be defined, for practical purposes, as one for which $\mathbf{r}$ approaches unity within acceptably close units. It is generally necessary that $\mathbf{r}$ lie between 0.90 and 1.10, and hence that

$$[(K^{II} - 1)(c_A)_o/C_o] < 0.10 \tag{137}$$

Thus, for a value of K^{II} large compared to unity, the peak value of c_A will need to be very small relative to C_o. For chromatographic separations under "trace" conditions, additional restrictions are sometimes necessary (V4).

For the trace-adsorption or trace-exchange case, $\mathbf{N}_R$ is unchanged from the "gross" value (Eq. 54), as given by Eq. (126). In this case, from Eq. (127),

$$\mathbf{Z} = \frac{1}{\mathbf{D}K^{II}} \frac{V - v\epsilon}{v\epsilon} \approx \frac{1}{\mathbf{D}_{trace}} \frac{V - v\epsilon}{v\epsilon}$$
$$\approx \frac{(c_A)_o(V - v\epsilon)}{(q_A)_o{}^*\rho_b v} \tag{138}$$

with $\mathbf{D}_{trace} = (q_A)_o{}^*\rho_b/(c_A)_o\epsilon$.

2. *External or Pore Diffusion Controlling*

From Eq. (19), (21), or (23), the equilibrium can be written:

$$\mathbf{x} = \frac{\mathbf{ry}}{1 + (\mathbf{r} - 1)\mathbf{y}} \tag{139}$$

For simple adsorption, or for exchange adsorption, Eq. (31) or (98) transforms to

$$\left(\frac{\partial \mathbf{y}}{\partial \mathbf{ZN}}\right)_{\mathbf{N}} = \mathbf{x} - \mathbf{x}^* \tag{140}$$

Introducing Eq. (139),

$$\left(\frac{\partial \mathbf{y}}{\partial \mathbf{ZN}}\right)_{\mathbf{N}} = \frac{\mathbf{x}(1 - \mathbf{y}) - \mathbf{ry}(1 - \mathbf{x})}{1 + (\mathbf{r} - 1)\mathbf{y}} \tag{141}$$

which corresponds to a result of Adamson and Grossman (A1, G8). This has the form of Eq. (35), and integrates to give Eq. (121), if

$$\mathbf{N}_R = \frac{\mathbf{N}}{1 + (\mathbf{r} - 1)\mathbf{y}} \tag{142}$$

where $\mathbf{N}$ is $\mathbf{N}_f$ or $\mathbf{N}_{pore}$. The average value of $\mathbf{y}$ may be taken as 0.5, if $\mathbf{r} < 1$; or as $1/(\mathbf{r} + 1)$, if $\mathbf{r} > 1$. Hence

$$\mathbf{N}_R = \frac{2\mathbf{N}_f}{\mathbf{r} + 1} \text{ or } \frac{2\mathbf{N}_{pore}}{\mathbf{r} + 1}, \text{ if } \mathbf{r} < 1 \tag{143}$$

$$\mathbf{N}_R = \frac{\mathbf{N}_f(\mathbf{r} + 1)}{2\mathbf{r}} \text{ or } \frac{\mathbf{N}_{pore}(\mathbf{r} + 1)}{2\mathbf{r}}, \text{ if } \mathbf{r} > 1 \tag{144}$$

With the use of these substitutions, the results tabulated for Eq. (121) can be used widely for diffusion-controlled rates. As will be discussed

in Section III, D, 4, Eq. (142) can be used without averaging y, if greater accuracy is needed.

3. *Solid-Phase (Internal) Diffusion Controlling*

The equilibrium can be written

$$y = \frac{x}{r + (1 - r)x} \tag{145}$$

Eqs. (37) and (145) give

$$\left(\frac{\partial y}{\partial Z N_p}\right)_{N_p} = y^* - y$$

$$= \frac{x(1 - y) - ry(1 - x)}{r + (1 - r)x} \tag{146}$$

This also integrates to give Eq. (121), if

$$N_R = \frac{N_p}{r + (1 - r)x} \tag{147}$$

For an average value of $x = 0.5$,

$$N_R = \frac{2N_p}{r + 1} \tag{148}$$

4. *Calculation for Non-Constant* N_R *or* r

If either of these parameters varies, the general reaction-kinetic solution can still be used to develop a breakthrough curve for any given pattern of behavior. An experimental curve may be divided into several regions, each of which is small enough for the correction factor to be essentially constant. In terms of curve-matching, this corresponds to matching different segments of a breakthrough curve to different master curves.

Based upon the equivalence of slopes at related points or within related small increments of the kinetic and the diffusional curves, the following procedure has been used in constructing the numerical plots of solutions of the diffusional equations (H6). The over-all concentration range is divided into four segments, as follows:

x, range, %	x_{avg}, %
1–10	3
10–50	30
50–90	70
90–99	97

Within each segment, the values of N_R and r are evaluated for the average x. From a reaction-kinetic plot of x vs. Z corresponding to an

appropriate $\mathbf{r}$, as calculated from Eq. (121), $\mathbf{Z}$ is read at the correct $\mathbf{N}_R$ for the concentrations at each end of the range, and a $\Delta\mathbf{Z}$ is computed. The latter values are plotted consecutively on linear-coordinate paper, and are integrated graphically, as by Eq. (73), to locate the $\mathbf{Z} = 1$ point and thus to establish the $\mathbf{Z}$ coordinates of the entire curve. Families of breakthrough curves for external and internal diffusion controlling, based on such constructions, are available (H6).

5. *Combined External-and Internal-Diffusion Resistances*

Under linear-equilibrium conditions, the combined effect of two diffusional resistances in series is treated by simple addition of the resistances. In the irreversible case, either the external or the internal resistance alone controls, with the latter over-taking the former part-way along the breakthrough curve (Section III, B, 2d). However, when the resistances are in relatively equal balance, with $3\mathbf{N}_p > \mathbf{N}_f > 0.3\mathbf{N}_p$, it is possible throughout the range of $\mathbf{r}$ values to calculate the breakthrough behavior by assuming an equivalent reaction-kinetic resistance.

It has been shown (H4) that the diffusional resistances can be combined by the relation:

$$\frac{\mathbf{b}\epsilon}{k_{kin}Q\rho_b} = \frac{1}{k_f a_p} + \frac{1}{k_p a_p \mathbf{D}} \tag{149}$$

Equation (38) provides the form of relation for expressing k_f. The exponent given there for N_{Se} was an assumed value, and experimental values are frequently nearer to -0.50. A simplified relation may therefore be written,

$$k_f = \alpha U(N_{Pe}')^{-0.50} \tag{150}$$

where $N_{Pe}' = d_p U\epsilon/6(1-\epsilon)D_f$ is the Peclet number for material transfer, and α is found empirically to be 0.38. With κ_{kin} replacing $k_{kin}Q\rho_b/\epsilon$, Eq. (149) becomes

$$\mathbf{b}\mathbf{D}\frac{D_p 6(1-\epsilon)}{d_p{}^2\kappa_{kin}} = \beta_1 \mathbf{D}\frac{D_p}{D_f}(N_{Pe}')^{-0.50} + \beta_2 \tag{151}$$

where $\beta_1 = \epsilon/6(1-\epsilon)\alpha$, and $\beta_2 = (1-\epsilon)/10$. This is the equation plotted in Fig. 6; and it is equivalent to Eq. (42) for a system of constant $\mathbf{b}$, $\mathbf{D}$ and ϵ.

The correction term $\mathbf{b}$ in Eqs. (149) and (151) is given by

$$\mathbf{b} = \frac{q_o^*(c - c_i) + C_o(q_i - q)}{c(q_o^* - q) - q(C_o - c)/K} \tag{152}$$

Since the interface concentrations c_i and q_i cannot be measured directly, a mechanism parameter which depends upon their behavior is also

defined:

$$\zeta = \frac{q_o^*(c - c_i)}{C_o(q_i - q)} \tag{153}$$

The relation between **b** and ζ is evaluated numerically by using successive assumed values of c_i (and q_i, in equilibrium with it) to determine both **b** and ζ. Usually c/C_o is taken as 0.5. In view of the low sensitivity of **b**

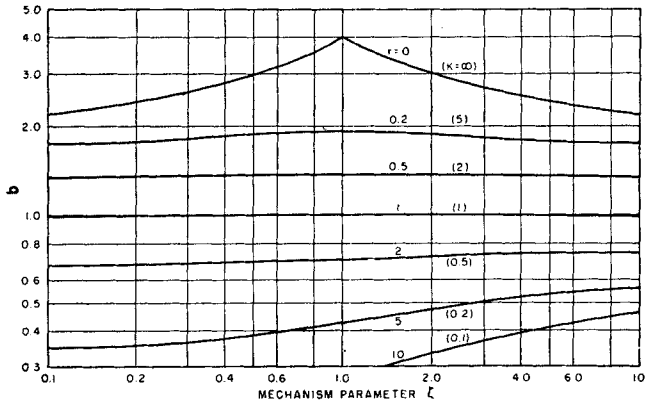

FIG. 9. Correction term for combining diffusional resistances. Courtesy of *A. I. Ch. E. Journal* (H4).

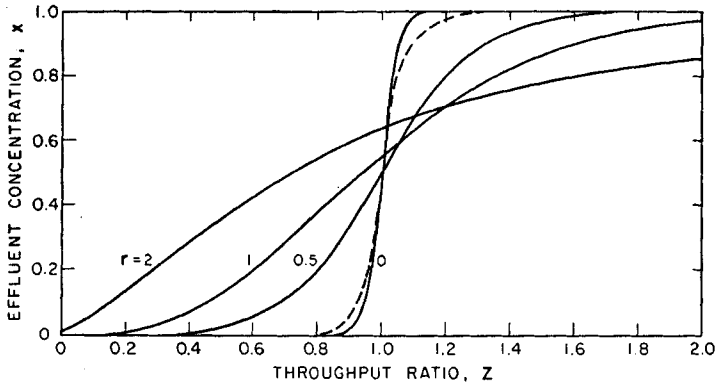

FIG. 10. Breakthrough curves at constant N_f and N_p, showing effect of changing equilibrium parameter **r**. At **r** = 0, the solid curve is given by the reaction-kinetic treatment (Eq. 96), and the dashed curve by the diffusional relations (Eqs. 79, 87, 94).

to changes in ζ, constant-pattern behavior is assumed for $K > 1$, with $c^*/C_o = 1/(1 + K)$; and proportionate-pattern behavior for $K < 1$, with $c^* \approx c$. Values of **b** calculated in this way are shown in Fig. 9.

Both in data interpretation and in equipment design, ζ must be evaluated from known or estimated mass-transfer coefficients or diffusivi-

ties, by the relations

$$\zeta = \mathbf{D}\frac{k_p}{k_f} = 4.8\mathbf{D}(\mathrm{N_{Re}}')^{-0.5}D_p/D_f \qquad (154)$$

Thus ζ is proportional to the abscissa of Fig. 6, and is shown in that figure on an auxiliary scale.

For calculating the over-all NTU's by Eqs. (52) and (53), the external-diffusion value $\mathbf{b}_f$ is given by $\mathbf{b}$ at the appropriate ζ, divided by $\mathbf{b}$ at $\zeta = \infty$. The internal diffusion value $\mathbf{b}_p$ is given by $\mathbf{b}$ at the appropriate ζ, divided by $\mathbf{b}$ at $\zeta = 0$.

From Eq. (149) it follows that

$$\frac{\mathbf{b}}{\mathbf{N}_R} = \frac{1}{\mathbf{N}_f} + \frac{1}{\mathbf{N}_p} = \frac{1}{\mathbf{N}_f}\frac{1+\zeta}{\zeta} = \frac{1+\zeta}{\mathbf{N}_p} \qquad (155)$$

At constant $\mathbf{N}_R$ and increasing $\mathbf{r}$ (decreasing K), the breakthrough curves become more shallow. At constant $\mathbf{N}_p$ and $\mathbf{N}_f$ as $\mathbf{r}$ increases, $\mathbf{N}_R$ will also decrease because of the behavior of $\mathbf{b}$; this intensifies the diminution in slope. Figure 10 gives a family of breakthrough plots for $\mathbf{N}_p = 20$ and $\mathbf{N}_f = 20$ at several $\mathbf{r}$ values, as calculated from the equivalent reaction-kinetic curves, and indicates a very great effect of equilibrium upon the concentration history.

E. Note on Multicomponent Saturation

The attention of many workers has been given to the equilibrium-limited case (proportionate-pattern) of multiple adsorption (D2, W1, W3, W7, among others). In the constant-pattern case, Fujita's work has already been discussed (Section III, B, 2b). Also, using the theoretical-plate approximation to a packed column, plate-by-plate calculations can be carried out in the constant-pattern case exactly as for continuous (countercurrent) distillation; this treatment is suggested from work on chromatographic and "displacement" problems by Mair (M2), Spedding (S6), and Glueckauf (G3). Moreover the linear-equilibrium result can be extended, in a nearly trivial fashion, to any number of components.

For the general multicomponent case of non-linear equilibrium, no calculation method has yet been developed for determining the rate-dependent, breakthrough behavior. An approximate calculation can be made by considering the feed mixture as a single component with an effective average $\mathbf{r}$, then estimating how the total adsorption wave (the terminology is from K4) will be divided into zones containing the individual components. With a feed containing two solutes, the one less strongly adsorbed will often over-ride the other and appear first in the

effluent; this behavior is utilized in the laboratory technique of *frontal analysis*, described by Tiselius (T3).

It is likely that progress in this field will come only after many additional data from column operations have been assembled systematically according to their respective rate and equilibrium values.

IV. Chromatographic Separations

A. General Principles

The essentials of chromatography have been discussed in Section I, A, and are illustrated in Fig. 1. Although saturation operations have been investigated at length by rate-theory approaches, the case of chromatographic elution from an incompletely saturated column has received little attention from the rate standpoint.

In the development of a chromatogram, or pattern of discrete solute zones, movement of each zone through the adsorbent occurs by the following mechanism. Fluid on the upstream (trailing) side of a zone is undersaturated with respect to the adsorbed component and continually takes it into solution. Passing beyond the peak of the zone to the downstream (leading) side, the same fluid is supersaturated relative to coexisting adsorbent and hence gradually redeposits the solute component.

A zone obeying a linear equilibrium would retain a constant rectangular shape, in the event that complete equilibrium could be maintained between solution and resin at each point in the column at all times during its elution. Actually, equilibrium cannot be maintained, and hence the zone undergoes a continual spreading; an initial rectangular shape changes to a flattened-top bell shape, and this in turn develops into a fully peaked bell shape.

A relative sharpening of each zone occurs as the length of column traversed increases, because the spreading of the zone is approximately proportional to the square root of the column length;[7] whereas the total volume of elutant[8] required, for complete elution of the zone, is almost directly proportional to the column length.

Vermeulen and Hiester have shown that the maximum useful charge to a column, in the linear-equilibrium case, will increase with the square root of column length.[9] Thus, at a constant flow rate, the volume of

[7] This is precisely so in the linear-equilibrium case ($\mathbf{r} = 1$). All other $\mathbf{r}$ values give somewhat more spreading.

[8] "Elutant" is preferred by the author and his co-workers for the agent effecting an elution; however, "eluent" and "elutriant" are also used by many writers.

[9] For ion exchange, in the non-trace case, the saturation step is assumed to be conducted at the same total fluid concentration C_0' as is used during the elution period. Under trace conditions, calculations can easily be made for $C_0 \neq C_0'$.

charge that can be processed per unit volume of adsorbent will be inversely proportional to the square root of column length. The systematic selection of optimum values of elutant concentration, pressure drop through the column, flow rate, total cycle period, charge period, recycle feed rate, multiple cycling, concentration of complexing agent, and number of stages of operation, has been analyzed for representative systems (V4, H2).

The feed may be introduced to the column as a narrow band of high (non-trace) concentration, as is customary in many laboratory separations. In elution, such a zone will first assume a flattened-top asymmetric

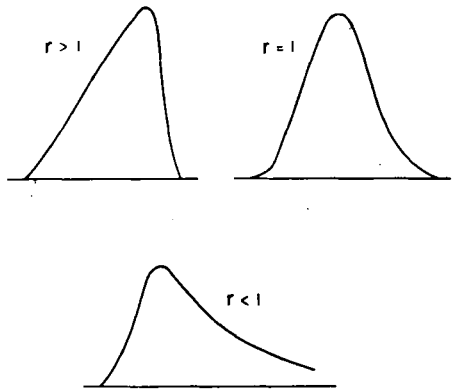

FIG. 11. Variation in symmetry of chromatograms. Ordinates represent concentration; abscissas, time. Courtesy of *Industrial and Engineering Chemistry.*

shape, then a peaked asymmetric shape, and ultimately, because of the reduction of the peak concentration level, a peaked symmetric shape consistent with trace conditions. It is observed that the optimum quantity of material that can be separated at maximum efficiency by a given column, when fed in this manner, is nearly identical with the optimum quantity of material fed under trace conditions (Section III, D, 1d) as an initially broader band of smaller amplitude. Further, the column behavior for a charge fed under non-trace conditions becomes nearly identical with that predicted by the comparatively simple calculation methods for fully trace conditions.

If $r = 1$, the concentration history for a chromatographic zone takes on a mirror-image symmetry with reference to its peak concentration, as the zone travels through a column of considerable length. Many asymmetric curves can therefore be attributed to deviations of r from unity—i.e., to non-trace conditions. It has been shown that the r values for a saturation and a corresponding elution are reciprocals of each other

(Section III, D, 1c). Also, for a column of given length, the smaller the value of $\mathbf{r}$ for saturation or for elution, the steeper is the saturation or elution curve.

If $\mathbf{r} < 1$ for saturation, the leading edge of the zone—the first to emerge in the effluent—will be steeper than the trailing edge; if $\mathbf{r} > 1$ for saturation, the leading edge will be more sloping than the trailing edge. Representative zone shapes for $\mathbf{r} < 1$, $\mathbf{r} = 1$, and $\mathbf{r} > 1$ are given in Fig. 11. Because $\mathbf{r}$ depends upon concentration, the symmetry or asymmetry of an elution curve for any component depends upon the maximum concentration levels of that component in the solution and on the resin, relative to the concentration levels of the carrier component.

In the trace case, the interactions between various solutes present can be neglected, provided not only that $c_A \ll C_o$ (or c_o^*), but also that $q_A \ll Q$. The non-trace case has been derived only for a single solute, in simple adsorption; or for a mixed feed of solute and eluting component, in exchange adsorption.

B. Single Chromatograms: Non-Trace Case

The method of surface-reaction kinetics at a constant separation factor, as developed by Thomas for saturation conditions, is again applied. Values of $\mathbf{N}_R$ should be calculated for the real or hypothetical saturation step, and for the elution step, by using the methods of Section III, D. An apparent NTU for saturation can be obtained from the calculated value for elution ($\mathbf{N}_R^\dagger$), by the relation $(\mathbf{N}_R)_{app} = \mathbf{N}_R^\dagger/\mathbf{r}$. Where part or all of the resistance is in the fluid phase, $(\mathbf{N}_R)_{app}$ will not be equal to $\mathbf{N}_R$ as determined for saturation; then, the combined saturation and elution should be described by the geometric mean of these two $\mathbf{N}_R$ values.

The equations derived in this section apply to either external or internal diffusion, or to both together, but probably not to longitudinal dispersion or diffusion as the controlling factor (as may occur particularly in gas chromatography). However, the equations of the next section, for "trace" chromatograms, should apply equally well regardless of which mechanism controls the shape to the curve.

A fluid containing the saturating component A, at concentration $(c_A)_o$, is considered to have passed through the column during a time interval τ_{sat}, which corresponds to a volume V_{sat} and a throughput ratio $\mathbf{Z}_{sat}$. At this instant, the eluting fluid begins to pass through the bed at an unchanged flow rate. This elutant stream differs from the previous fluid only in the omission of saturating component (or in replacement of saturant by additional eluting component to keep C_o constant).

Equations (35) and (68) have been solved in this case by Hiester and

Vermeulen (H1, H5) and by Goldstein (G6). The boundary conditions are:

$$\text{At } v = 0,\ \lambda = c_A/(c_A)_o = 0$$
$$\text{At } Z' = 0, \text{ as a function of } Z_{sat} \text{ and } N_R,$$

$$\omega = \frac{q_A}{(q_A)_o^*} = \frac{1 - J(Z_{sat}N_R, rN_R)}{J(rN_R, Z_{sat}N_R) + e^{(r-1)N_R(Z_{sat}-1)}[1 - J(N_R, rZ_{sat}N_R)]} \quad (156)$$

The resulting equations are

$$\lambda' \text{ (denom.)} = J(rN_R, ZN_R) - J(rN_R, Z'N_R) \quad (157)$$
$$\omega' \text{ (denom.)} = J(Z'N_R, rN_R) - J(ZN_R, rN_R) \quad (158)$$

where

$$\text{(denom.)} = J(rN_R, ZN_R) + e^{(r-1)N_R(Z-1)}[1 - J(N_R, rZN_R)] + e^{(r-1)N_R(Z'-1)}[1 - J(rZ'N_R, N_R)] + J(Z'N_R, rN_R) - 1 \quad (159)$$

where the unprimed values are measured from the start of the saturation period, and the primed values (′) from the start of the elution period. It can be shown that, for large values of Z_{sat}, these equations will reduce to the form for elution from a completely saturated bed (Section III, D, 1). This limit will occur near $Z_{sat} = 2\sqrt{\pi/N_R}$.

A discontinuity in fluid concentration will occur at the assumedly sharp elutant front. As the front travels down the bed, this discontinuity decreases and rapidly becomes negligible.

The function Z_{sat} can be described as a "memory" term. Equations for multiple saturation and elution involving more than one memory term are also given by Hiester (H1).

Goldstein (G6) has provided approximation functions to aid in evaluating Eqs. (157–159). Baddour and co-workers (B1) have demonstrated their utility for matching experimental curves. For example, with $r < 1$ and $Z_{sat} < 1 - r$, the following rules apply: Below $Z = Z_{sat} + r$, λ' is given by x from Eq. (96); and above $Z = 1/r$, from Eq. (75). Between these two limits, Goldstein finds

$$\frac{1}{\lambda'} = \frac{1 - r}{(r/Z)^{1/2} - r} - (4\pi N_R)^{1/2}(rZ)^{1/4}[1 - (Z'/r)^{1/2}]e^{N_R[(\sqrt{rZ'}-1)^2-(1-r)Z]} \quad (160)$$

The elution of two non-trace solutes (H^+, K^+) by a third component (Na^+) has been studied by Baddour and Hawthorn, under conditions where the equilibrium constant for exchange was less than unity between one component (H^+) and the elutant, and this component was eluted first; while the equilibrium constant for the other component was greater than one. Equations (157–160) were found to apply, provided the leading band (H^+) was calculated as if its inlet concentration were that of

both solute components (H^+ plus K^+); with V_{sat} in the calculations, reduced in value to correspond to the total amount of H^+ actually introduced. For the trailing band, the concentration curve could be calculated just as if the leading component had not been present. The extension of this method to related situations awaits further experimental study.

C. "Trace" Chromatograms (Linear Equilibrium)

1. *Exact Treatment*

The value of trace conditions for obtaining sharp separations has been discussed in Section IV, A, and the criteria in terms of K^{II} and $(c_A)_o/C_o$ are given in Eqs. (136), (137), and (29). As already stated, "trace" conditions are characterized especially by a value of the equilibrium parameter $\mathbf{r}$, equal to unity.

From two different approaches, Stene (S7), and Rosen and Winsche (R2) have shown that the sequence of saturation and elution can be described by the difference between the concentration curve for saturation starting at $\mathbf{Z} = 0$ and continuing through the elution period, and a second curve representing non-existent saturant which starts at $\mathbf{Z}' = 0$. Vermeulen and Hiester (V4) have demonstrated that, with $\mathbf{r} = 1$, Eq. (157) shows just this property:

$$\lambda' = c_A/(c_A')_o = \mathbf{J}(\mathbf{N}_R,\mathbf{Z}\mathbf{N}_R) - \mathbf{J}(\mathbf{N}_R,\mathbf{Z}'\mathbf{N}_R) \qquad (161)$$

Figure 12 shows the transition from complete saturation to incomplete saturation that occurs, at $\mathbf{r} = 1$ and $\mathbf{N}_R = 80$, as $\mathbf{Z}_{sat}$ is progressively reduced. Boyd and co-workers (B8) and Glueckauf (G4) have also considered the chromatogram as a composite of separate saturation and elution curves.

For maximum utilization of adsorbent, it is desirable to select a charge period which will give λ_{max} between 0.50 and 0.85; thus, as will be shown, $\mathbf{Z}_{sat}$ should be between $\sqrt{\pi/\mathbf{N}_R}$ and $\sqrt{3\pi/\mathbf{N}_R}$. At λ_{max} values below 0.50, the same quantity of adsorbent serves to recover smaller amounts of solute. At still higher $\mathbf{Z}_{sat}$ values, on the other hand, the overlap between successive solute components increases so that the utilization of adsorbent levels off and gradually declines.

2. *Gaussian-Shaped Zones*

The lower two curves of Fig. 12 are seen to be symmetrical, and similar in shape to each other. Such curves can be represented by a Gaussian-distribution equation, provided that (a) $\mathbf{N}_R > 50$, and (b) $\mathbf{Z} < \sqrt{\pi/\mathbf{N}_R}$.

Equation (109) can be used with the last term neglected, at high $\mathbf{N}_R$. With the introduction of Eq. (110), Eq. (161) becomes:

$$c_A'/(c_A')_o = \tfrac{1}{2} \operatorname{erf} \sqrt{N_R}\,(\sqrt{Z} - 1) - \operatorname{erf} \sqrt{N_R}\,(\sqrt{Z'} - 1)$$
$$= \int_{\sqrt{N_R}(\sqrt{Z'}-1)}^{\sqrt{N_R}(\sqrt{Z}-1)} e^{-\eta^2}\, d\eta \qquad (162)$$

If the upper limit is close to the lower limit, the theorem of the mean allows the integral to be approximated by the product of an intermediate value of its integrand, multiplied by the interval of the independent

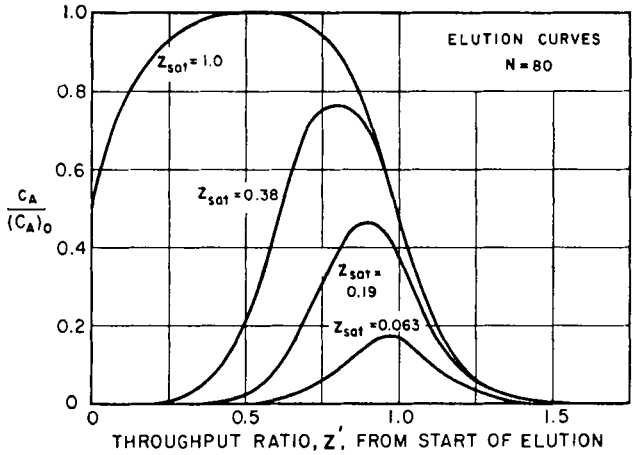

FIG. 12. Elution curves for varying charge periods.

variable. A suitable intermediate value of the variable, η, is taken at the midpoint of the interval. Thus

$$\frac{c_A'}{(c_A')_o} = \frac{\sqrt{N_R}\,(\sqrt{Z} - \sqrt{Z'})}{\sqrt{\pi}}\, e^{-N_R(0.5\sqrt{Z}+0.5\sqrt{Z'}-1)^2} \qquad (163)$$

Further transformation (V4) gives

$$\frac{c_A'}{(c_A')_o} = \frac{Z_{sat}\sqrt{N_R}}{2\sqrt{\pi}}\, e^{-(N_R/4)(Z'+0.5Z_{sat}-1)^2} \qquad (164)$$

Glueckauf (G4) has obtained a similar result.

The peak of the zone is given by

$$(c_A')_{max} = (c_A')_o Z_{sat}\sqrt{N_R}/2\sqrt{\pi}$$
$$= \frac{\sqrt{N_R}\,[(c_A)_o V_{sat}]}{2\pi[V'_{max} + 0.5(C_o/C_o')V_{sat} - v\epsilon]} \qquad (165)$$

where V'_{max} is the volume of elutant that has entered the column when the peak is reached; $V'_{max} = (D'_{trace} + 1)v\epsilon$, different for each solute.

The shape of the zone is given by

$$\ln \frac{(c_A')_{max}}{c_A'} = \frac{\mathbf{N}_R}{4}(\mathbf{Z}' + 0.5\mathbf{Z}_{sat} - 1)^2$$
$$= \frac{\mathbf{N}_R}{4}\left(\frac{V' - V'_{max}}{V'_{max} + 0.5(C_o/C_o')V_{sat} - v\epsilon}\right)^2 \quad (166)$$

This relation is used to evaluate $\mathbf{N}_R$ from the half-width of the zone, measured at the half-height or the $1/e$ height.

Mayer and Tompkins (M6), and Matheson (M5) have used the theoretical-plate approach to derive

$$\ln \frac{(c_A')_{max}}{c_A'} = \frac{N_o}{2}\left(\frac{\mathbf{D}'_{trace} + 1}{\mathbf{D}'_{trace}}\right)\left(\frac{V' - V'_{max}}{V'_{max}}\right)^2 \quad (167)$$

where N_o is the number of equilibrium contacts, in accordance with Mayer and Tompkins's definition of a theoretical plate. At large $\mathbf{D}_{trace}$,

$$\mathbf{N}_R = 2N_o \quad (168)$$

Thus the number of equilibrium stages is directly proportional to column length, if the linear flow rate remains unchanged. The role of contact time, which is obscured in the plate theory, now becomes evident. Wherever mass-transfer is independent of flow rate, a diminution of the flow velocity through a bed of constant length will increase the effective number of theoretical plates in inverse proportion. The number of plates in any one column may vary for the different components, just as $\mathbf{N}_R$ may, although usually the variation is not great.

The correspondence between $\mathbf{N}_R$ and N_o makes it possible to transform all the relations developed for reaction units or transfer units into calculations for theoretical plates. Nevertheless, the theoretical-plate approach is based upon a much less precise model, and is applicable to fixed beds only in special cases (such as linear equilibrium, or constant pattern). Like many approximations, the theoretical-plate method is generally derived and applied without exact knowledge of its limitations.

3. *Design of "Trace" Separations*

To separate two or more solutes by chromatography, in a pilot-plant unit designed for maximum economy, the operating conditions will generally be established in the following order (V4):

a. The adsorbent composition will be selected, along with the levels of concentration (or partial pressure), that give the greatest difference in distribution ratio ($\mathbf{D}'_{trace}$) values for the different components.

b. The average charge rate of feed mixture is considered a fixed condition. This may be based on a trace component which is present in largest quantity, or whose equilibrium parameter, $\mathbf{r}$, is farthest from

unity. It will be expressed as moles fed per unit time; or, when divided by the concentration in the charge, as an average volumetric charge rate.

c. The recovery requirements and $\mathbf{D}_{trace}$ values, together, determine the $\mathbf{N}_R$ values for each component. For each component whose concentration follows a Gaussian curve, the **J**-function curve has a new use: it represents the integrated recovery of material at the appropriate $\mathbf{N}_R$ and $(\mathbf{Z})_{apparent}$ (or $\mathbf{Z}' + 0.5\mathbf{Z}_{sat}$).

When the ratios of $\mathbf{D}'_{trace}$ values (for short, **D**) and of $\mathbf{N}_R$ values (for short, **N**) for two components A and B are known, the **J** curves can be used to relate $\mathbf{N}_R$ values to the degree of separation in the following way:

i. Let A represent the component with lower **D**, which is thus eluted first. The maximum allowable loss of A into fractions containing B is specified; the remaining A will all be recovered ahead of this point.

ii. At an ordinate on Fig. 8 numerically equal to the recovery of A, read for any assumed $\mathbf{N}_A$ the corresponding $\mathbf{Z}_A$.

This value must be multiplied by the ratio $\mathbf{D}_A/\mathbf{D}_B$ to determine $\mathbf{Z}_B$. Also $\mathbf{N}_A$ must be converted to the corresponding $\mathbf{N}_B$.

iii. At the values of $\mathbf{N}_B$ and $\mathbf{Z}_B$ thus calculated, the ordinate on Fig. 8 is read. This gives the loss of B into fractions containing A.

iv. If the recovery of B is greater than required, assume a smaller $\mathbf{N}_A$ and repeat. Conversely, if it is insufficient, assume a larger $\mathbf{N}_A$.

v. *Use of recycle.* A moderate reduction in $\mathbf{N}_R$, and hence also in resin volume, may be obtained by taking a low recovery of A per pass at the requisite purity. A separate cross-contaminated fraction containing both A and B can then be collected for recycling in a subsequent portion of feed, before taking the B fraction.

vi. *Multiple cycling.* Whenever the separation factors are close to unity, the components undergoing separation will occupy only a small part of the column at any one time. If, in a single cycle of adsorption and elution, the portions of effluent containing trace components comprise less than half the total volume of effluent, as occurs in many binary separations, the utilization of the resin can be improved by adsorbing a second feed charge from a solution of the same carrier composition as the elutant, before elution of the first charge has been completed. In this way, the effluent can become an almost continuous succession of trace zones.[10] Figure 13 shows a schedule of multiple cycling proposed for a radium-barium separation (V4).

d. The volumetric flow rate is then determined. $(\mathbf{Z}_A)_{sat}$ is taken as $\sqrt{\pi/\mathbf{N}_A}$. The total $\mathbf{Z}_A$ in one cycle is calculated as $\mathbf{D}_Z/\mathbf{D}_A$ times the $\mathbf{Z}_Z$

[10] Multiple cycling is not feasible in cases of *graded elution*, which involve a progressive change in elutant composition; for such a case, however, this entire calculation procedure must be modified substantially.

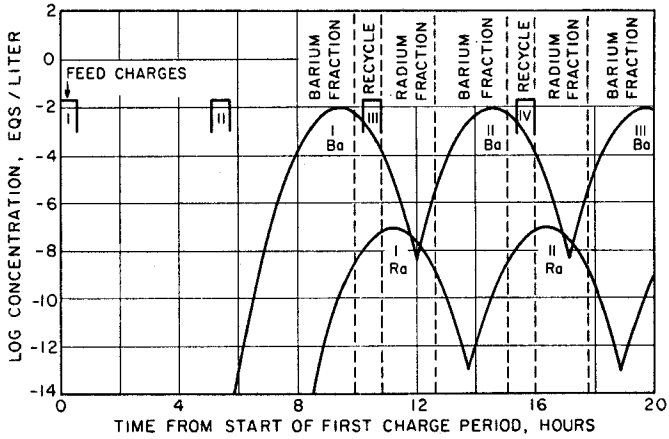

FIG. 13. Effluent composition predicted for first column of a radium-barium separation process.

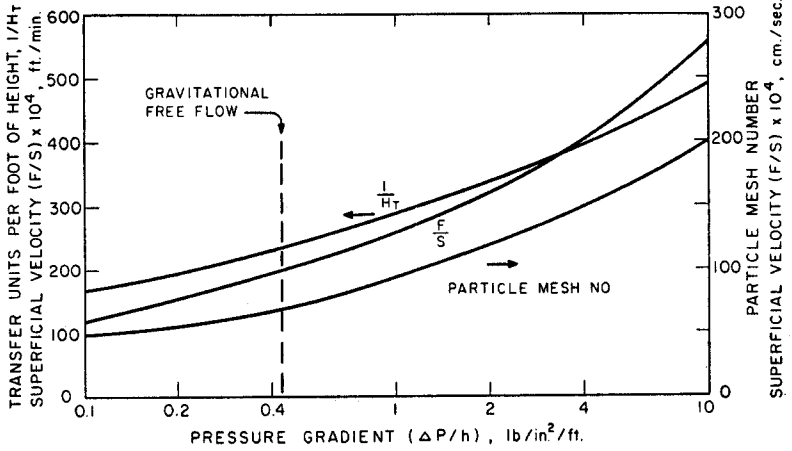

FIG. 14. Typical relation of operating variables for ion exchange or liquid-phase adsorption. Courtesy of *Industrial and Engineering Chemistry*.

required to elute completely the last component (Z) in the column. The total flow rate F is then given by

$$F = \frac{(Z_A)_{total}}{(Z_A)_{sat}} \times (\text{volumetric charge rate}) \qquad (169)$$

e. The column volume and the cycle period remain to be specified. It will be desirable, for liquid-phase adsorptions at least, to use N_{Pe}' as near as is practicable to 20, but no lower because of the onset of longitudi-

nal diffusion. This variation in N_{Pe}' is accomplished by decreasing the particle volume, with an attendant increase in pressure drop per unit height. Figure 14 shows the relations between d_p, $\mathbf{N}_R$, $\Delta P/h$, and F/S calculated for a representative instance of ion exchange.

The linear flow rate U assumed here, together with the known volumetric flow F, fixes the cross-sectional area S.

Once the range of economic N_{Pe}' values has been selected, Fig. 6 can be used to determine κ_{kin} for the component on which calculations are based. By Eq. 54, with $\kappa_{kin} = k_{kin}Q\rho_b/\epsilon$, the column volume is

$$v = \mathbf{N}_R F/\kappa_{kin}\epsilon \tag{170}$$

From S and v, the length of the column is now established. Several trial calculations will usually be needed to achieve the most economical bed geometry.

Nomenclature

a constant of integration, in Eq. 71
a_p effective mass-transfer area between fluid and particles, ft.²/ft.³ (or cm.²/cm.³)
A, B, G, Z components
A, B, C coefficients in power-series isotherm (Eqs. 12–13)
c concentration of solute in the fluid phase, lb.-mole or lb.-equiv./ft.³ (or gm.-mole or gm.-equiv./cm.³)
c heat capacity
C_o total concentration of solutes in the fluid phase
d_p diameter of sphere equal in volume to actual particle, ft. (or cm.)
D diffusivity, ft.²/hr. (or cm.²/sec.)
E effective longitudinal dispersivity, ft.²/hr. (or cm.²/sec.)
F volumetric flowrate, ft.³/hr. (or cm.³/sec.)
g Brinkley's function; see Eq. (107)
H height of contact volume equivalent to one transfer unit or reactor unit, ft. (or cm.)
I_o Bessel function of zero order with imaginary argument; see Eq. (105)
k rate coefficient for kinetics (ft.³/hr. lb.-mole, or cm.³/sec. gm.-mole)
K equilibrium constant for exchange or adsorption, in appropriate concentration or pressure units
l axial depth of a radial bed
l, m, n exponents
L, M exponents
L symmetric Margules factor for activity-coefficient expression (Eq. 15)
M molecular weight
n integer in infinite series (Eq. 81)
N mole fraction
N_o number of equivalent contacts (theoretical plates)
N_{Pe}' Peclet number for mass transfer, $N_{Re} \times N_{Sc}$, dimensionless
N_{Re} Reynolds number for flow past particles, $d_pU\epsilon\rho/6(1-\epsilon)\mu$, dimensionless

N_{Sc} Schmidt number, $\mu/D\rho$, dimensionless
p partial pressure of solute
P vapor pressure, lb.-force/ft.^{2} (or gm.-force/cm.^{2})
q concentration of solute in the particle phase, lb.-mole or lb.-equiv./lb. (or gm.-mole or gm.-equiv./gm.) of air dried particles
Q ultimate exchange capacity of the particle phase; equivalent to q_m, for adsorption
r radial distance within spherical particle, ft. (or cm.)
r_p radius of exterior surface of particle, ft. (or cm.)
$\bar{r}$ average pore radius, ft. (or cm.)
R radial distance within adsorbent bed
S cross-sectional area of contactor, ft.^{2} (or cm.^{2})
s, t variables in the argument of J analogous to s, t
$\bar{u}$ average molecular velocity, ft./hr. (or cm./sec.)
U actual mean linear flow rate of fluid phase relative to solid, ft./hr. (or cm./sec.)
v bulk-packed volume for contact, ft.^{3} (or cm.^{3})
V volume of saturating feed entering column, ft.^{3} (or cm.^{3})

J mathematical solution for column-saturation function; gives x at r = 1
n number of effective transfer units with longitudinal dispersion; see Eq. (113b)
N number of transfer units; see Eqs. (50–51)
N_H number of heat-transfer units; see Eq. (117)
N_R number of reaction units; see Eq. (54)
r equilibrium parameter
s column-capacity parameter for fixed-bed operation, based on reaction-kinetics calculation
t solution-capacity parameter for fixed-bed operation, based on reaction-kinetics calculation
x ratio of fluid-phase concentration of a component to that of all components, c/C_o (x_A, etc.)
y ratio of particle-phase concentration of a component to total for solid at saturation with the feed, q/Q
z modified throughput ratio for longitudinal dispersion; see Eq. (113a)
Z throughput parameter, or ratio of actual volume of effluent to the stoichiometric volume; t/s or Θ/Σ

Dimensionless Parameters

b correction factor for computing overall mass-transfer, or rate, coefficients
D distribution parameter, or ratio of concentrations in particle and fluid phases

Greek Letters

α, β valence of ions A, B
$\alpha_1, \alpha_2, \beta_1, \beta_2$ correlation constants for mass-transfer
γ activity coefficient
ϵ ratio of void space outside particles to total volume of contacting zone

ζ mechanism parameter
Θ solution capacity parameter, based on mass-transfer calculation
η a variable, in Eqs. (110) and (162)
κ_{kin} general rate coefficient in the reaction-kinetic equation; $k_{kin}Q\rho_b/\epsilon$; hr.$^{-1}$ (or sec.$^{-1}$)
λ extent of saturation of fluid phase with reference to initial and final concentrations; $[x_A - (x_A)_o^*]/[(x_A)_o - (x_A)_o^*]$
μ viscosity of the fluid, lb./hr. ft. (or gm./cm. sec.)
ξ a variable, in Eq. (105)
ρ density, lb./ft.^{3} (or gm./cm.^{3}), usually the fluid density; ρ_b = bulk-packed density of air-dried particles
Σ column-capacity parameter for fixed-bed operation, based on mass-transfer calculation
τ time, hr. (or sec.)
ϕ Thomas's function; see Eq. (106)
χ internal porosity of solid particles
ψ numerical correction factor for solid-phase diffusion, Eq. (86)
ω extent of saturation of particle phase with reference to initial and final concentrations; $[y_A - (y_A)_o]/[(y_A)_o^* - (y_A)_o]$

SUBSCRIPTS

1, 2, . . . instantaneous times of measurement
app apparent
B, C, F, L, S types of adsorption equilibria
b bulk
b boundary value for special case of Eq. (87)
complex formation of complex ion
d distribution
e exterior
f fluid phase
i interior
i interface
H heat transfer
kin reaction-kinetic
m monomolecular layer
max value at the peak of the chromatogram
O over-all
o initial or entrance conditions
p particle phase
pore fluid phase pore diffusion
R reaction unit
sat increment during saturating period
stoic stoichiometric proportions
T total
trace trace conditions
∞ value when pores are filled with condensed liquid
∞ temperature of fluid at saturation

SUPERSCRIPTS

$*$ equilibrium
$'$ second time interval in binary saturation or elution
$'$ adsorption equilibrium involving a liquid phase
$\dagger$ elution period following complete saturation
II equal-valence exchange

REFERENCES

A1. Adamson, A. W., and Grossman, J. J., *J. Chem. Phys.* **17**, 1002 (1949).
A2. Amundson, N. R., *J. Phys. & Colloid Chem.* **54**, 812 (1950).

A3. Anzelius, A., *Z. angew. Math. u. Mech.* **6,** 291 (1926).
A4. Aris, R., and Amundson, N. R., *A. I. Ch. E. Journal* **3,** 280 (1957).
B1. Baddour, B. F., Goldstein, D. J., and Epstein, P., *Ind. Eng. Chem.* **46,** 2192 (1954); Baddour, B. F., and Hawthorn, R. D., *ibid.* **47,** 2517 (1955).
B2. Barrer, R. M., "Diffusion in and through Solids." Cambridge Univ. Press, London and New York, 1941.
B3. Barrow, R. F., Danby, C. J., Davoud, J. G., Hinshelwood, C. N., and Staveley, L. A. K., *J. Chem. Soc.* p. 401 (1947).
B4. Bauman, W. C., and Eichhorn, J., *J. Am. Chem. Soc.* **69,** 2830 (1947).
B5. Beaton, R. H., and Furnas, C. C., *Ind. Eng. Chem.* **33,** 1500 (1941).
B6. Bohart, G. S., and Adams, E. Q., *J. Am. Chem. Soc.* **42,** 523 (1920).
B7. Boyd, G. E., and Soldano, B. A., *J. Am. Chem. Soc.* **75,** 6091, 6107 (1953).
B8. Boyd, G. E., Myers, L. S., Jr., and Adamson, A. W., *J. Am. Chem. Soc.* **69,** 2836, 2849 (1947).
B9. Boyd, G. E., Schubert, J., and Adamson, A. W., *J. Am. Chem. Soc.* **69,** 2818 (1947).
B10. Brinkley, S. R., Jr., Edwards, H. E., and Smith, R. W. Jr., *Math. Tables Aids Computation* **6,** 40 (1952).
B11. Brownell, L. E., and Katz, D. L., *Chem. Eng. Progr.* **43,** 537 (1947); also in Brown, G. G., "Unit Operations," Chapter 16. Wiley, New York, 1950.
B12. Brunauer, S., "Physical Adsorption," Princeton Univ. Press, Princeton, New Jersey, 1943.
B13. Brunauer, S., Emmett, P. H., and Teller, E., *J. Am. Chem. Soc.* **60,** 309 (1938).
B14. Brunauer, S., Deming, L. S., Deming, W. E., and Teller, E., *J. Am. Chem. Soc.* **62,** 1723 (1940).
C1. Caddell, J. R., and Moison, R. L., *Chem. Eng. Progr. Symposium Ser.* **50,** No. 14, 1 (1954).
C2. Cassidy, H. G., "Adsorption and Chromatography," Vol. V of "Technique of Organic Chemistry." Interscience, New York, 1951.
C3. Chilton, T. H., and Colburn, A. P., *Ind. Eng. Chem.* **27,** 255 (1935).
D1. DeVaney, F. D., *in* "Chemical Engineers' Handbook" (J. H. Perry, ed.), pp. 1085–1091. McGraw-Hill, New York, 1950.
D2. DeVault, D., *J. Am. Chem. Soc.* **65,** 532 (1943).
D3. Dodge, F. W., and Hougen, O. A., "Drying of Gases," Edwards, Ann Arbor, Michigan, 1947.
D4. Drew, T. B., and Genereaux, R. P., *in* "Chemical Engineers' Handbook" (J. H. Perry, ed.), pp. 393–394. McGraw-Hill, New York, 1950.
D5. Drew, T. B., Spooner, F. M., and Douglas, J., cited in reference (K4).
D6. Dryden, C. E., Ph.D. thesis in chemical engineering. Ohio State University, Columbus, Ohio, 1951.
E1. Eagleton, L., and Bliss, H., *Chem. Eng. Progr.* **49,** 543 (1953).
E2. Einstein, H. A., D.S.T. dissertation, Eidgenössische Technische Hochschule, Zürich, Switzerland, 1937.
E3. Ergun, S., *Chem. Eng. Progr.* **48,** 227 (1952).
F1. Fredericks, E. M., and Brooks, F. R., *Anal. Chem.* **28,** 297 (1956).
F2. Fujita, H., *J. Phys. Chem.* **56,** 949 (1952).
F3. Furnas, C. C., *Trans. Am. Inst. Chem. Engrs.* **24,** 142 (1930).
G1. Gaffney, B. J., and Drew, T. B., *Ind. Eng. Chem.* **42,** 1120 (1950).
G2. Gilliland, E. R., and Baddour, R. F., *Ind. Eng. Chem.* **45,** 330 (1953).
G3. Glueckauf, E., *Trans. Faraday Soc.* **51,** 1540 (1955).
G4. Glueckauf, E., *J. Chem. Soc.* p. 1302 (1947); *Discussions Faraday Soc.* **7,** 12

(1949); *Trans. Faraday Soc.* **51,** 34 (1955); Glueckauf, E., Barker, K. H., and Kitt, G. P., *ibid.* p. 199 (1949).
G5. Glueckauf, E., and Coates, J. I., *J. Chem. Soc.* p. 1315 (1947).
G6. Goldstein, S., *Proc. Roy. Soc.* **A219,** 151, 171 (1953).
G7. Gregor, H. P., *J. Colloid Sci.* **6,** 20 (1951).
G8. Grossman, J. J., and Adamson, A. W., *J. Phys. Chem.* **56,** 97 (1952).
H1. Hiester, N. K., Ph.D. dissertation in chemical engineering, University of California, Berkeley, Calif., 1949.
H2. Hiester, N. K., Cohen, R. K., and Phillips, R. C., *Chem. Eng. Progr. Symposium Ser.* **50,** No. 14, 23 (1954).
H3. Hiester, N. K., Cohen, R. K., and Phillips, R. C., *Chem. Eng. Progr. Symposium Ser.* **50,** No. 14, 63; also *Chem. Eng. Progr.* **50,** 139 (1954).
H4. Hiester, N. K., Radding, S. B., Nelson, R. L., Jr., and Vermeulen, T., *A. I. Ch. E. Journal* **2,** 404 (1956); *Am. Documentation Inst.* Doc. 4953 (1956).
H5. Hiester, N. K., and Vermeulen, T., *J. Chem. Phys.* **16,** 1087 (1948).
H6. Hiester, N. K., and Vermeulen, T., *Chem. Eng. Progr.* **48,** 505 (1952); *Am. Documentation Inst.* Doc. 3665 (1952).
H7. Hougen, O. A., and Marshall, W. R., *Chem. Eng. Progr.* **43,** 197 (1947).
H8. Hurt, D. M., *Ind. Eng. Chem.* **35,** 522 (1943).
J1. Jacques, G., and Vermeulen, T., *Univ. Calif. Radiation Lab. Rept.* 8029 (1957).
K1. Kasten, P. R., Lapidus, L., and Amundson, N. R., *J. Phys. Chem.* **56,** 683 (1952).
K2. Keulemans, A. I. M., "Gas Chromatography." Reinhold, New York, 1957.
K3. Klinkenberg, A., *Ind. Eng. Chem.* **40,** 1970 (1948); **46,** 2285 (1954).
K4. Klotz, I. M., *Chem. Revs.* **39,** 241 (1946).
K5. Koble, R. A., and Corrigan, T. E., *Ind. Eng. Chem.* **44,** 383 (1952).
K6. Kramers, H., and Alberda, G., *Chem. Eng. Sci.* **2,** 173 (1953).
K7. Kunin, R., and Myers, R. J., "Ion-Exchange Resins." Wiley, New York, 1950.
L1. Langmuir, I., *Phys. Revs.* **2,** 331 (1913); *ibid.* **6,** 79 (1915); *J. Am. Chem. Soc.* **38,** 2221 (1916).
L2. Lapidus, L., and Amundson, N. R., *J. Phys. Chem.* **54,** 821 (1950); **56,** 373 (1952).
L3. Lapidus, L., and Amundson, N. R., *J. Phys. Chem.* **56,** 984 (1952); Amundson, N. R., *Ind. Eng. Chem.* **48,** 26 (1956).
L4. Ledoux, E., *J. Phys. & Colloid Chem.* **53,** 960 (1949).
M1. McCune, L. K., and Wilhelm, R. H., *Ind. Eng. Chem.* **41,** 1124 (1949).
M2. Mair, B. J., Westhaver, J. W., and Rossini, F. D., *Ind. Eng. Chem.* **42,** 1279 (1950).
M3. Mantell, C. L., "Adsorption," 2nd ed. McGraw-Hill, New York, 1951.
M4. Martin, A. J. P., and Synge, R. L. M., *Biochem. J.* **35,** 1385 (1941).
M5. Matheson, L. A., private communication, reported by Tompkins, E. R., *J. Chem. Educ.* **26,** 92 (1949).
M6. Mayer, S. W., and Tompkins, E. R., *J. Am. Chem. Soc.* **69,** 2866 (1947).
M7. Michaels, A. S., *Ind. Eng. Chem.* **44,** 1922 (1952).
M8. Miyauchi, T., Ph.D. dissertation, University of Tokyo, Japan, 1957.
N1. Nachod, F. C., ed., "Ion Exchange: Theory and Application." Academic Press, New York, 1949.
N2. Nelson, R. L., Jr., M.S. thesis in chemical engineering, University of California, Berkeley, Calif., 1951.
O1. Opler, A., and Hiester, N. K., "Tables for Predicting the Performance of Fixed-Bed Ion Exchange and Similar Mass Transfer Processes." Stanford Research Institute, Stanford, Calif., 1954.
R1. Rosen, J. B., *J. Chem. Phys.* **20,** 387 (1952); *Ind. Eng. Chem.* **46,** 1590 (1954).

R2. Rosen, J. B., and Winsche, W. E., *J. Chem. Phys.* **18,** 1587 (1950).
S1. Schumann, T. E. W., *J. Franklin Inst.* **208,** 405 (1929).
S2. Selke, W. A., and Bliss, H., *Chem. Eng. Progr.* **46,** 509 (1950).
S3. Shedlovsky, L., *Ann. N.Y. Acad. Sci.* **49,** 279 (1938).
S4. Sillén, L. G., *Arkiv Kemi Mineral. Geol.* **A22,** No. 15 (1946); Sillén, L. G., and Ekedahl, E., *ibid.* **A22,** No. 16 (1946).
S5. Sips, R., *J. Chem. Phys.* **18,** 1024 (1950).
S6. Spedding, F. H., and Powell, J. E., *J. Am. Chem. Soc.* **76,** 2550 (1954).
S7. Stene, S., *Arkiv Kemi Mineral. Geol.* **18,** No. 18 (1945).
T1. Thomas, H. C., *J. Am. Chem. Soc.* **66,** 1664 (1944).
T2. Thomas, H. C., *Ann. N.Y. Acad. Sci.* **49,** 161 (1948).
T3. Tiselius, A., *Advances in Colloid Sci.* **1,** 81 (1942).
T4. Treybal, R. E., "Mass-Transfer Operations." McGraw-Hill, New York, 1955.
V1. Van Arsdel, W. B., *Chem. Eng. Progr.* **43,** 13 (1947).
V2. Van Deemter, J. J., Zuiderweg, F. J., and Klinkenberg, A., *Chem. Eng. Sci.* **5,** 271 (1956).
V3. Vermeulen, T., *Ind. Eng. Chem.* **45,** 1664 (1953).
V4. Vermeulen, T., and Hiester, N. K., *Ind. Eng. Chem.* **44,** 636 (1952).
V5. Vermeulen, T., and Hiester, N. K., *J. Chem. Phys.* **22,** 96 (1954).
V6. Vermeulen, T., and Huffman, E. H., *Ind. Eng. Chem.* **45,** 1658 (1953).
W1. Walter, J. E., *J. Chem. Phys.* **13,** 229 (1945).
W2. Walton, H. F., in reference (N1).
W3. Weiss, J., *J. Chem. Soc.* p. 297 (1943); Offord, A. C., and Weiss, J., *Discussions Faraday Soc.* **7,** 26 (1949).
W4. Wheeler, A., *Advances in Catalysis* **3,** 250–327 (1951); "Catalysis," Vol. 2 (P. H. Emmett, ed.) pp. 105–165: Reinhold, New York (1955).
W5. Wicke, E., *Kolloid-Z.* **86,** 167, 289 (1939).
W6. Wilke, C. R., and Hougen, O. A., *Trans. Am. Inst. Chem. Engrs.* **41,** 445 (1945).
W7. Wilson, J. N., *J. Am. Chem. Soc.* **62,** 1583 (1940).
W8. Wilson, S., and Lapidus, L., *Ind. Eng. Chem.* **48,** 992 (1956).